THE UNIVERSITY OF HULL

Synthesis and characterization of Schiff-base complexes as medical imaging precursors

Being a Thesis submitted for the Degree of

Master of Science by Research

at the University of Hull

December 2018

By

Sultan Abdullah A Alqarni

BSc. KAU

Master of Diagnostic Radiography, USyd

Abstract

Schiff-base compounds have been utilized in the medical field as antibiotics, antifungal, anti-inflammatory and antiviral agents. The presence of nitrogen, oxygen and sulphur atoms in chelating Schiff-base compounds showed great biological activities. Furthermore, their derivative metal complexes have exhibited greater effects in many reported cases. Some Schiff-base complexes have been reported as medical imaging agents. The aim of my work is to synthesis novel Schiff base ligands and their metal derivatives that have the potential to be used as medical imaging precursors. A novel macrocyclic Schiff-base ligand was developed from 3,5-diformyl-4-hydroxybenzoic acid and 2,2'-oxydianiline. Also, a novel crystal structure for a known macrocyclic Schiff-base was synthesized from 2,2'-oxydianiline and 4-*tert*-butyl-2,6-diformylphenol. Finally, a novel copper Schiff-base complex synthesized.

Acknowledgements

First and foremost, I would like to thank God Almighty for giving me the durability, capacity and opportunity to commence this research study.

I would like to thank my supervisor, Professor Carl Redshaw, for everything he offered from the beginning. His brilliant insights helped me through the difficulties I have faced since the start of journey.

I am thankful to the supporting staff of chemistry in the University of Hull, specially Carol Kennedy in the elemental analysis department for her help. Also special thanks Dr David L Hughes at the University of East Anglia and Dr Mark Elsegood at the Loughborough University for collecting crystallography data.

A special thanks to the government of Saudi Arabia for every kind of support I received through my educational journey through the University of Taif and the Cultural Bureau in London.

In addition, I would like to thank my friends Mohammed Alamri, Abdullah Alshamrani, Tian Xing, Kuiyan Wang and Yahya Alkhafaji, for their consistent support and help.

Last but not least, I am greatly thankful to my parents and family, whom without this journey would have been much harder. Their continuing patience, understanding, support and encouragement gave me the strength I needed during this research.

List of abbreviations

ROP	Ring opening polymerization
Me	Methyl group
t-Bu	*Tert*-butyl
Et	Ethyl group
Bu^i	Isobutyl
ROS	Reactive oxygen species
SPECT	Single photon emission computed tomography
PET	Positron emission tomography
MeOH	Methanol
EtOH	Ethanol
DMF	Dimethylformamide
HCl	Hydrochloric acid
mAbs	Monoclonal antibodies
SOD	superoxide dismutase
mmol	Millimoles
ml	millilitre
^oC	Degree centigrade
mg	Milligram
g	Gram
cm^3	Cubic centimetre
DMF	Dimethylformamide
Å	Angstrom
^oC	Degree Celsius

List of figures

List of schemes

List of tables

Contents

Chapter 1

Introduction

1.1 Chemistry of Schiff-base compounds

Named after its inventor, Hugo Schiff, Schiff-base compounds are denoted by the double bond between a carbon atom and a nitrogen atom. An alkyl or aryl group is usually connected to the nitrogen rather than hydrogen. In general, the formula of Schiff-base compounds is $R^1R^2C{=}NR^3$ (figure 1), where R^3 is an organic side chain.[1]

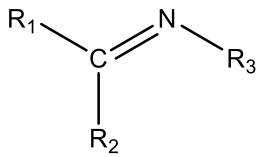

Figure 1. Basic structure of Schiff base compounds.

The nitrogen connected chain is the one responsible for making the Schiff base stable imines. There is also a Schiff base which is acquired from aniline and in this case the R^3 is a phenyl or a substituted phenyl.[1] The formation of a Schiff base occurs when any primary amine reacts with an aldehyde or a ketone but only when certain conditions are met. In the structural perspective, the Schiff base which is additionally known as imines or azomethines is a nitrogen analogue of a ketone or an aldehyde where carbonyl group represented by C=O is substituted with an imine or azomethine group. The Schiff base also happens to be one of the most common organic compounds that are in use. Compounds belonging to this category often show analgesic, anti-inflammatory, non-ulcerogenic and antimicrobial features.[102]

Naturally, Schiff-base compounds appear to be oily or crystalline. They are soluble in organic solvents but usually insoluble in water. As they are classified as week bases, when reacted with acids in anhydrous environment they produce salts. On the other hand, when placed in aqueous solutions they undergo hydrolysis forming aldehydes or amines. In alkaline solutions, most Schiff-base compounds are stable. In organic synthesis, Schiff-base compounds are very important intermediate products. For example, in chemical reactions that make secondary amines and various heterocyclic compounds. Also, azomethine dyes are Schiff-base compounds that can be utilised in dyeing synthetic fibres and acetate. Some Schiff-base compounds are vital for minimizing photosensitivity of photographic emulsions in colour photography.[101]

1.2 Organometallic Schiff-base complexes

Schiff-base ligands have the potential to form organometallic complexes with any metal ion.[3] There are many Schiff-base organometallic complexes that have great catalytic activity and are vital to increase product yield and selectivity. The fairly easy synthesis route and the thermal stability of Schiff-base ligands are very important in their utilization in catalysis as organometallic complexes.[4]

Another functional group adjacent to the imine function group is present in many Schiff-base ligands. Generally, this second functional group is hydroxyl. This is very important when coordinating metal ions as the closeness of these two functional groups to each other allows the formation of up to six chelate rings.[5]

Numerous Schiff-base metal complexes were developed in recent years to be used in ring opening polymerization (ROP). In 2016, W. Yang *et al.*, developed seven Schiff-base manganese macrocyclic complexes (figures 2-7)[6]. Most of the Schiff-base ligands were able to accommodate two manganese centres. These complexes were used for the ROP of ε-caprolactone as pre-catalysts. The results showed that these Schiff-base manganese complexes were not suitable for ROP of ε-caprolactone.[6]

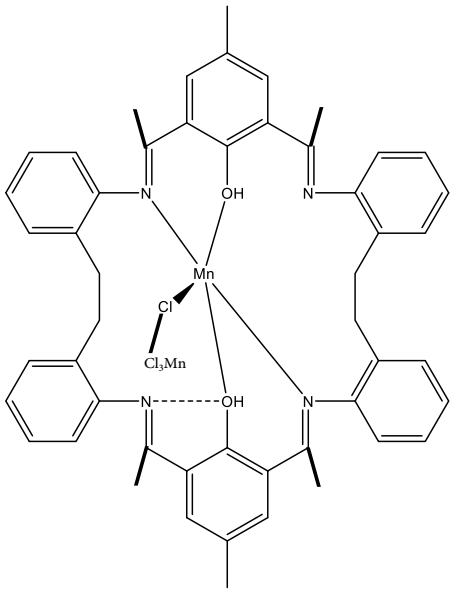

Figure 2. First manganese Schiff-base macrocyclic complex developed by W. Yang et al. [6]

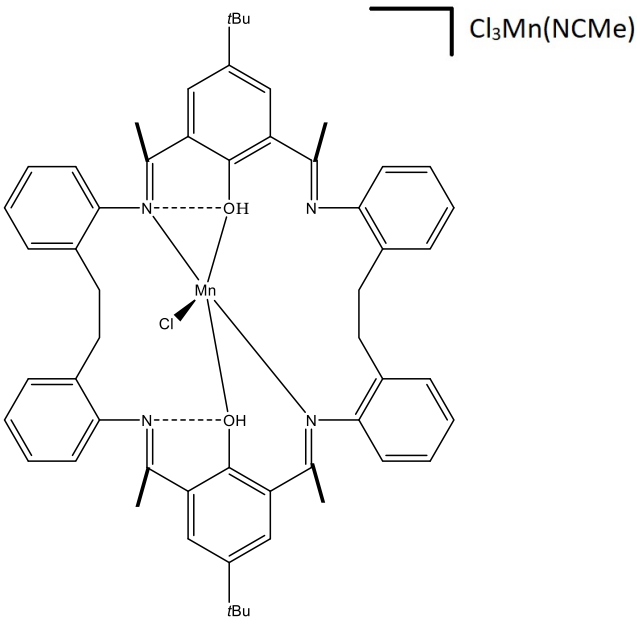

Figure 3. Second manganese Schiff-base macrocyclic complex developed by W. Yang et al.[6]

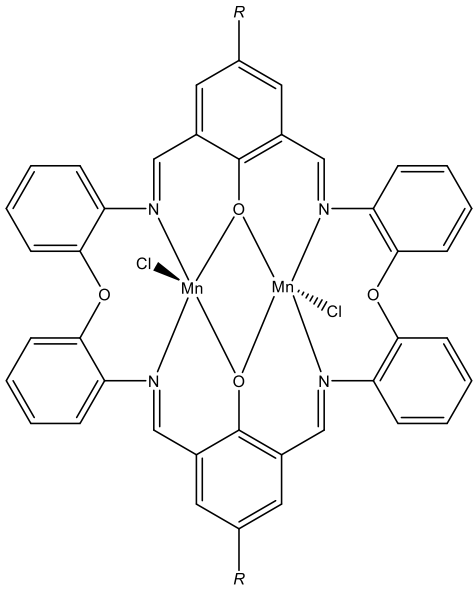

Figure 4. Third and fourth manganese Schiff-base macrocyclic complex developed by W. Yang et al. [6] (R=Me or t-Bu)

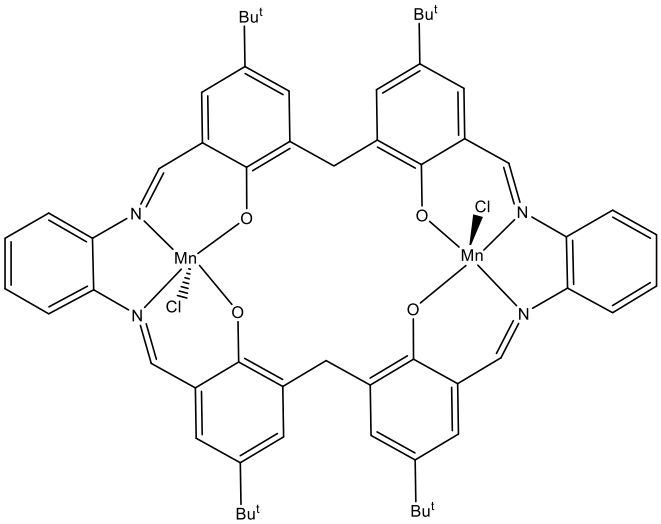

Figure 5. Fifth manganese Schiff-base macrocyclic complex developed by W. Yang et al. [6]

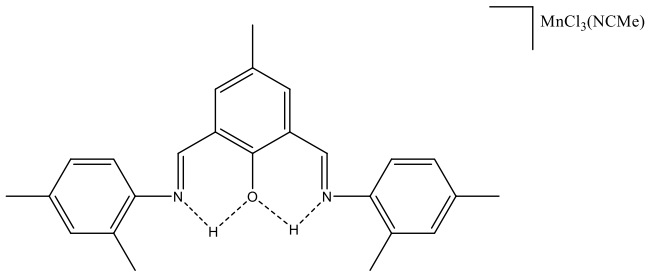

Figure 6. Sixth manganese Schiff-base macrocycle developed by W. Yang et al. [6]

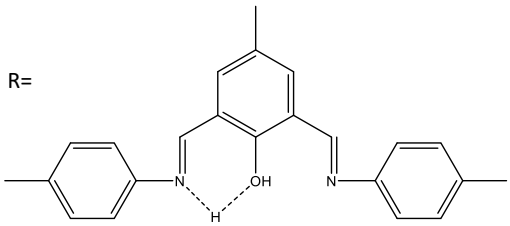

Figure 7. Seventh manganese Schiff-base macrocycle [Mn(R)2(μ-Cl)]2[$MnCl_4$] developed by W. Yang et al. [6]

The research group published that same year another paper about the synthesis of 14 new Schiff-base macrocyclic aluminium complexes (figure 8). These complexes were used in the ROP of ε-caprolactone and rac-lactide. The study concluded that all the new Schiff-base macrocyclic complexes were not very beneficial in ROP of ε-caprolactone and rac-lactide under the employed conditions.[7]

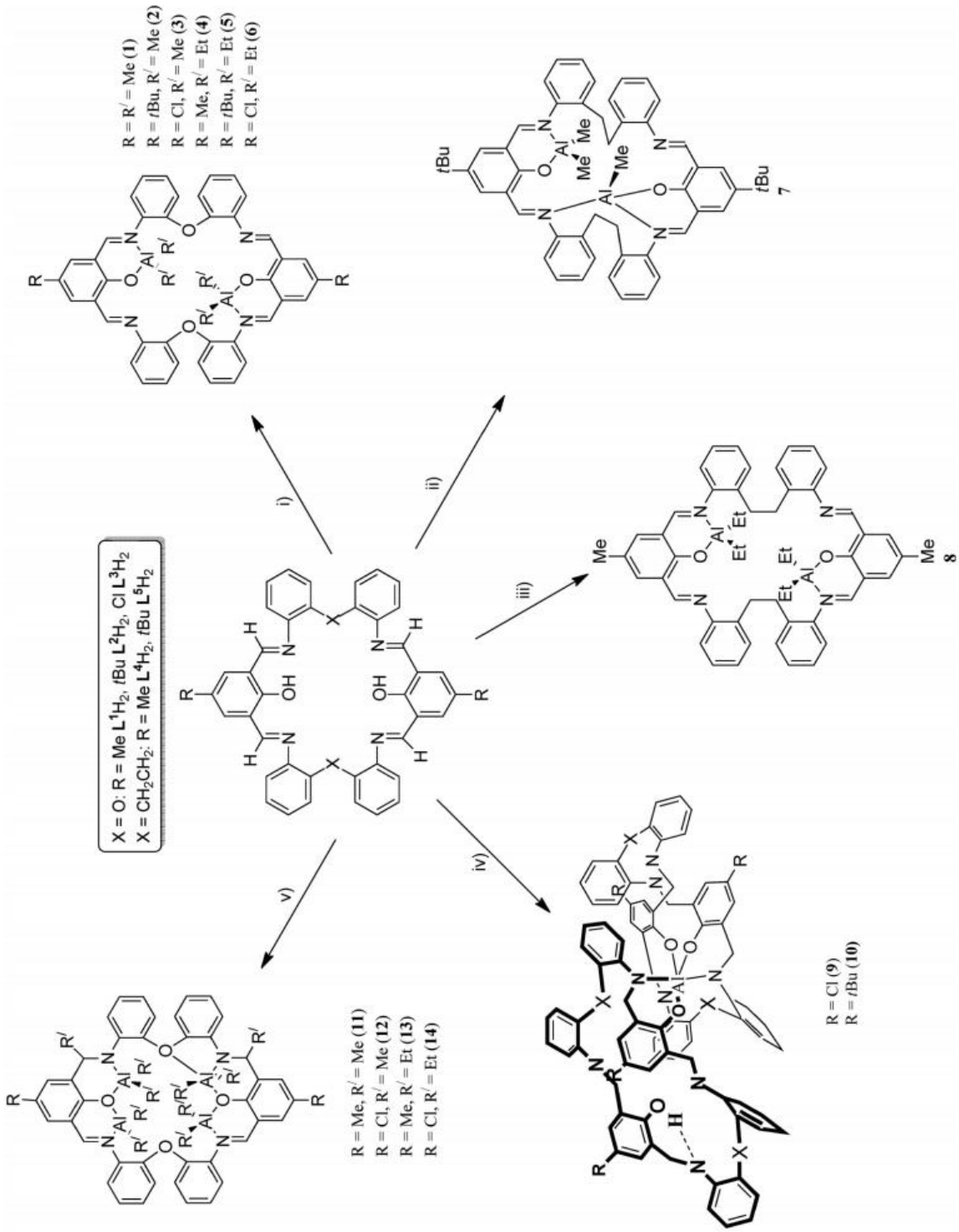

Figure 8. Aluminium Schiff-base macrocyclic complexes.[7]

In 2017, Yang, *et al.* made eleven new aluminium Schiff-base complexes (figure 9). These complexes were used in the ROP of ε-caprolact-one, δ-valerolactone and rac-lactide, in which these complexes were active. In addition, with reasonable lactide incorporation, these complexes were able to co-polymerize ε-caprolactone/rac-lactide.[8]

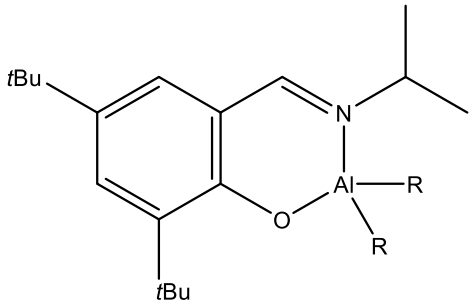

(R=Me or Et)

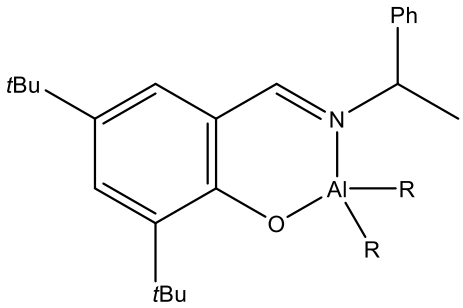

(R=Me or Et)

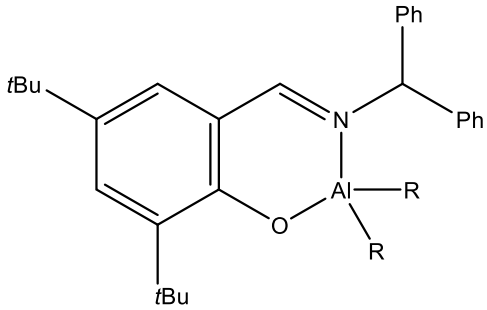

R=Me or Et)

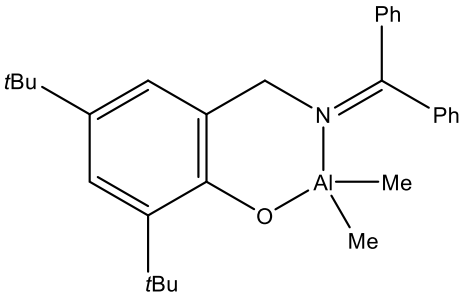

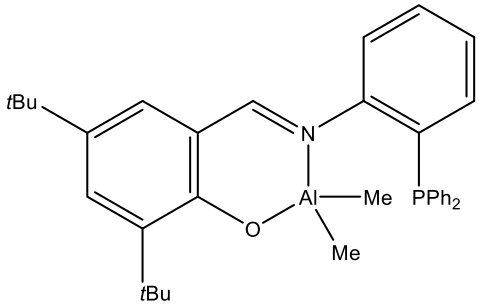

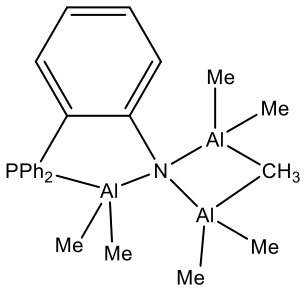

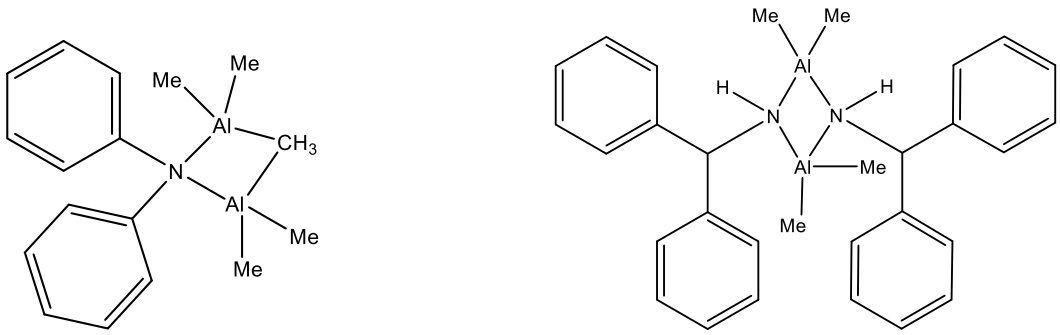

Figure 9. Aluminium Schiff-base complexes developed by Yang *et al.*[8]

1.3 Schiff Bases in medicine

Because of its antifungal, anticancer, antibacterial, anti-inflammatory and antiviral properties, Schiff-base metal complexes have been extensively studied.[9] Chelating ligands with nitrogen, sulphur and oxygen donating atoms, as the case with Schiff-base ligands, display wide biological activity and are interesting due to the various ways metal ions bond to them. The presence of a metal bonded to these ligands improve their activities.[10, 11]

1.3.1 Antibacterial Schiff bases

Schiff base metal complexes made from 2-aminobenzoic acid and 2-thiophene carboxaldehyde and Fe(III), Ni(II) or Co(II) (figure 10) demonstrated decent antibacterial action against Pseudomonas aeruginosa, Escherichia coli and Staphylococcus pyogenes. The Zn(II), Cu(II) and Fe(III) complexes led to the inhibition of the E. coli. This means that these complexes have the potential to be used in the treatment of some common E. coli caused diseases. On the other hand, Cu(II), Fe(III), Zn(II) and Co(II) complexes specialized in inhibiting Staphylococcus pyogenes and P.

aeruginosa (Gram-positive bacterial strains). These Schiff-base complexes can be safely used to treat infections induced by these bacteria strains.[12]

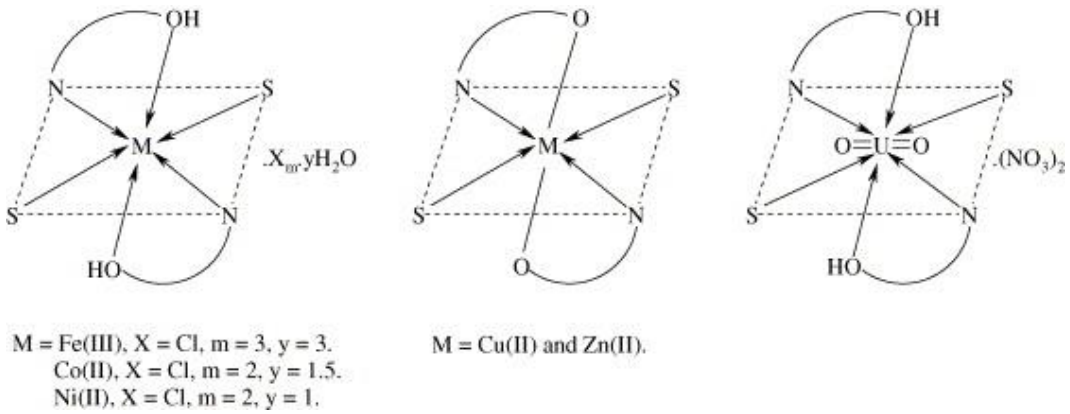

Figure 10. Structural formulae of Schiff-base complexes.[12]

In 2007, Gaballa *et al.* reported four platinum(II) Schiff-base complexes that contain 2-furaldehyde and salicylaldehyde with o- and p-phenylenediamine to be antibacterial towards Bacillus subtilis, E. coli, P. aeruginosa and Staphylococcus aureus. Research data demonstrated that these complexes were more effective than their Schiff-based parent ligands towards at least one microorganism.[13]

Novel Schiff-base metal complexes synthesized by condensation of varelaldehyde and sulphametrole were tested on E. coli and S. aureus bacterial species. These Schiff-base ligand and their metal derivatives demonstrated greater impact on S. aureus (Gram-positive bacteria) and E. coli (Gram-negative bacteria).[14] Gram negative bacteria membrane is covered by an outer membrane that contains lipopolysaccharides. The prepared Schiff-base ligands and their metal complexes appeared to be able to integrate with outer membrane which enhanced the Gram-negative bacteria's membrane permeability. Lipophilicity is an important factor that controls the activity of the antimicrobial due to the lipid nature of the membrane that surrounds the Gram-nigative bacteria.[15-17] The Schiff bases and their metal derivatives were more toxic towards S. aureus than they were on E. coli, most likely because of their sulfonic OH, OCH_3, CH_3CH_2CH and S groups, that have the potential to interact with that double membranes.[14]

1.3.2 Antifungal Schiff bases

In 2008, Neelakantan *et al.* reported cobalt(II), nickel(II), copper(II) and manganese(II) Schiff-base complexes (figure 11) were tested on three fungi. The nickel(II) and copper(II) complexes exhibited inhibition against all microorganisms involved in the study. On the other hand, the cobalt(II) and manganese(II) showed lower inhibition towards those microorganisms.[18]

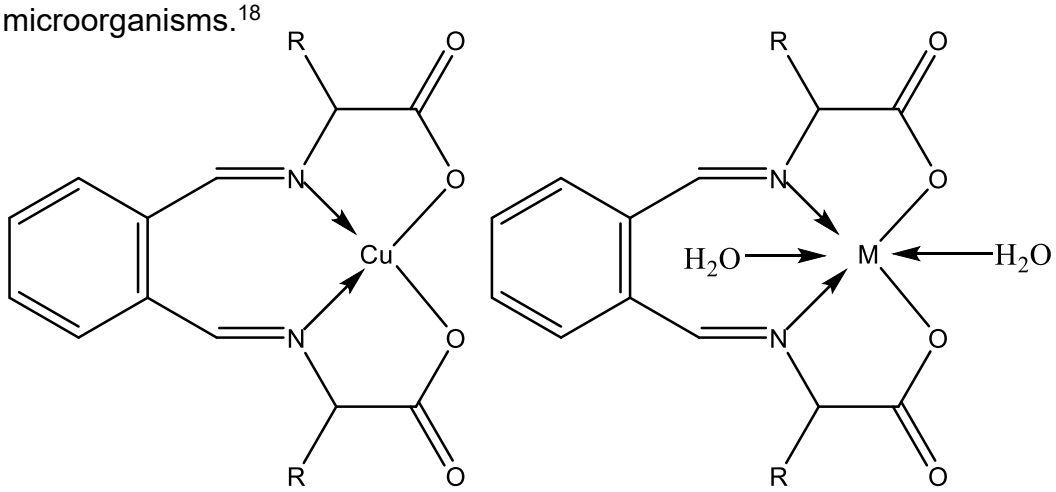

Figure 11. Cobalt(II), nickel(II), copper(II) and manganese(II) Schiff-base complexes. R= H, CH_3, C_6H_6.

In 2012, Kumar *et al.* reported making chromium(III), manganese(III) and iron(III) Schiff-base complexes (scheme 1) which were tested to show their inhibitory potential as antimicrobials. The results were compared to same concentrations of Miconazole, the standard antifungal drug. When tested against Aspergillus sp., the metal complexes showed higher antifungal activity than Miconazole. On the other hand, they showed lower activity than Miconazole when tested on Rhizoctonia sp. In addition, when tested on

Penicillium sp., the chromium(III) and the iron(III) Schiff-base complexes were more effective than Miconazole.[19]

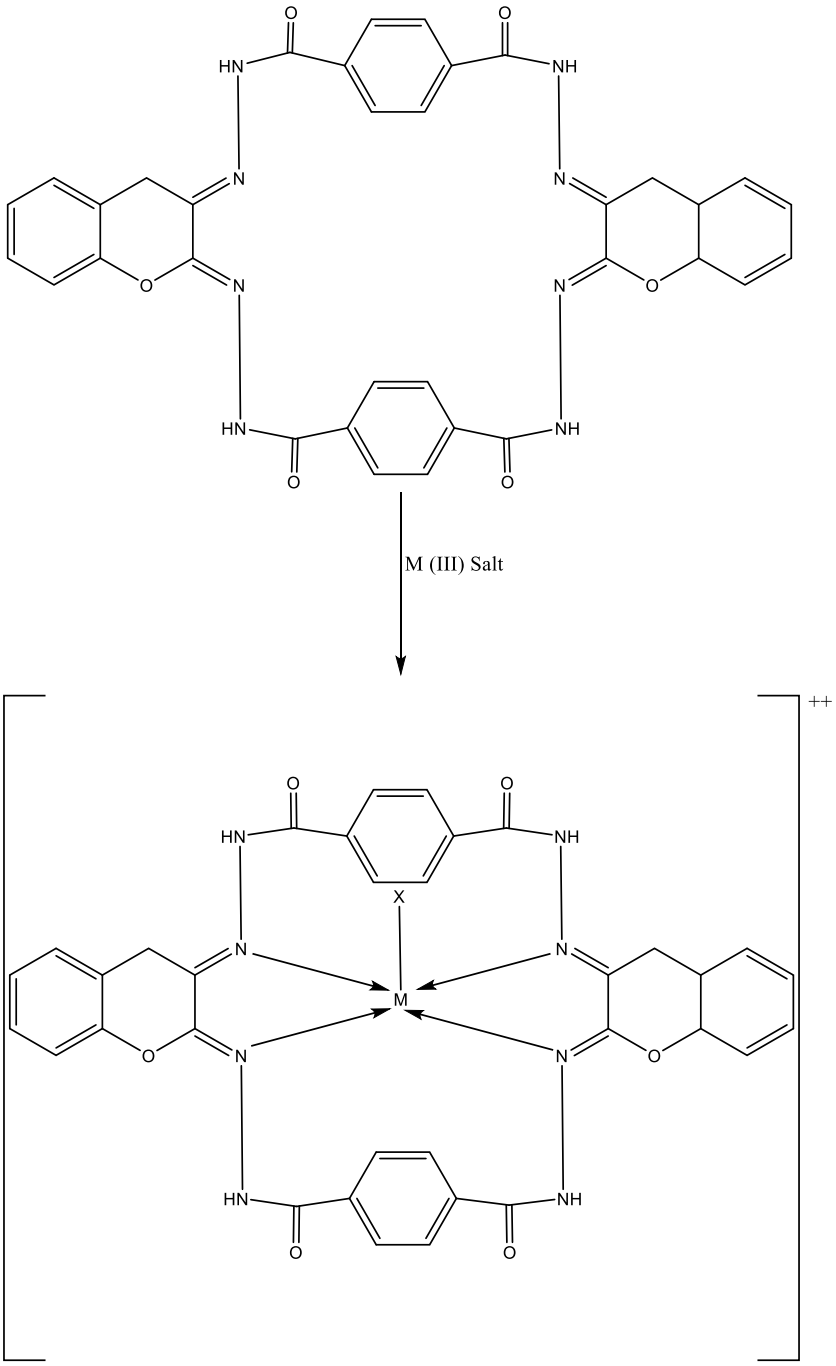

Scheme 1. Chromium(III), manganese(III) and iron(III) Schiff-base complexes.

X=Cl^-,NO_3^- or CH_3COO^-.

1.3.3 Anti-inflammatory Schiff bases

In 2008, Pontiki *et al.*, synthesized a series of novel copper (II) Schiff-base complexes. These Schiff-base complexes anti-inflammatory and antioxidant activities were tested. The results showed inhibition of carrageenin-induced rat paw oedema by the tested complexes. They also exhibited scavenging activity. The complex $[(C_4H_4)CHNCH_2CH_2]_2NHCuY_2$(2a-5mt) showed more activity than it starting material $[(C_4H_4)CHNCH_2CH_2]_2NHCuY_2$(figure 12). [20]

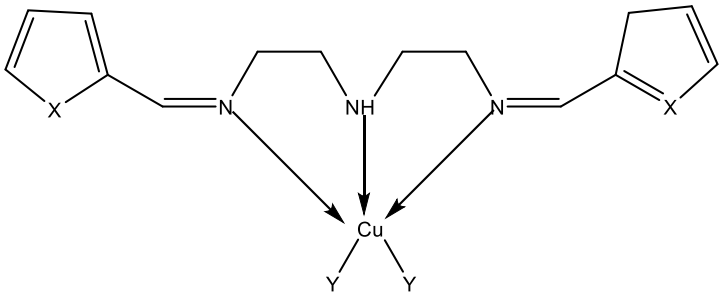

$[(C_4H_4X)CHNCH_2CH_2]_2NHCuY_2$

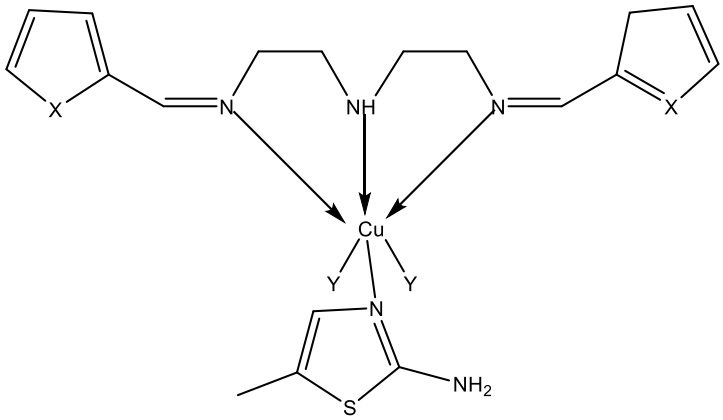

$[(C_4H_4X)CHNCH_2CH_2]_2NHCuY_2$(2a-5mt)

Figure 12. $[(C_4H_4X)CHNCH_2CH_2]_2NHCuY_2$(2a-5mt) and it starting material $[(C_4H_4X)CHNCH_2CH_2]_2NHCuY_2$

X= O or S.

Y=Cl, Br or NO_3.

1.3.4 Antiviral Schiff base complexes

Viral infections have many therapeutic options, however, they are not entirely effective most likely because of the increased rate of mutations of viruses. Among various types of 1-amino-3-hydroxyguanidine tosylate-derived Schiff-base compounds (scheme 2, table 1), the 2-(3-allyl-2-hydroxybenzylidene)-*N*-hydroxyhydrazinecarboximidamide derivative was the most effective towards hepatitis virus in mice (MHV) by inhibiting the virus growth by fifty percent at concentrations as little as 3.2 μM.[21]

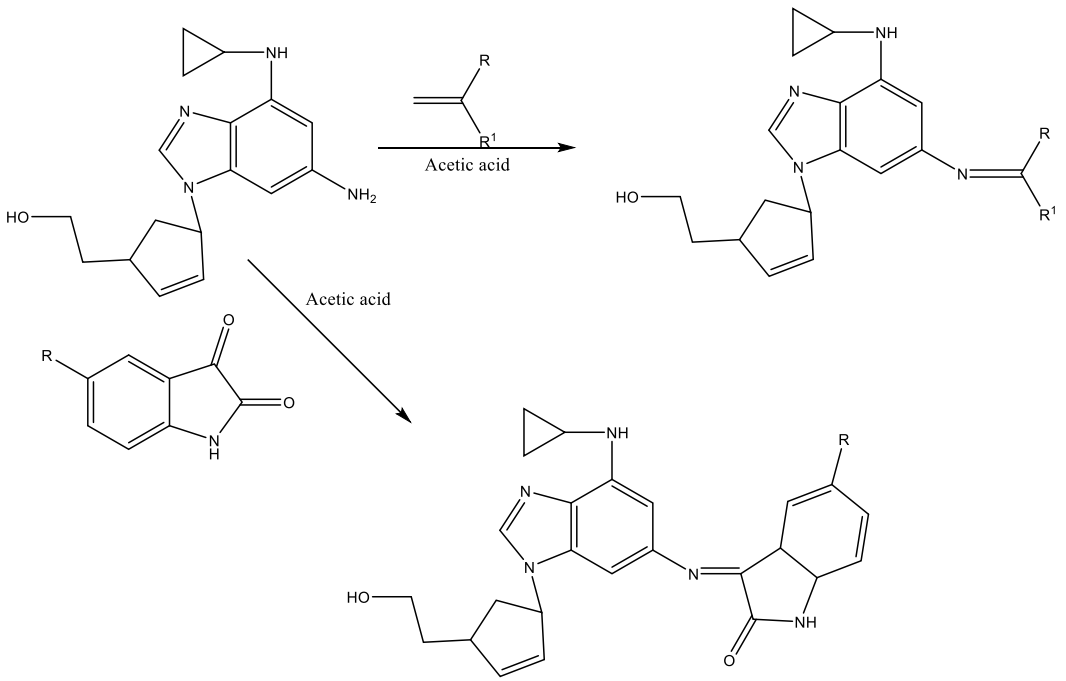

Scheme 2. Synthesis of Schiff-base compounds developed by Sriram *et al*.[21]
R and R^1 groups are shown in table 1.

Table 1. R and R^1 groups in the Schiff-base compounds developed by Sriram *et al.*[21]

Compound	**R**	**R^1**
1	H	2-Nitro phenyl
2	H	4-Nitro phenyl
3	H	4-Methyl phenyl
4	H	4-Methoxy phenyl
5	H	4-dimethylaminophenyl
6	H	2-Hydroxy-4-methoxy phenyl
7	CH_3	4-Hydroxy phenyl
8	C_6H_6	4-Bromo phenyl
9	H	_____
10	F	_____
11	CH_3	_____

In 2010, Kumar *et al.*, developed a new set of 3-(benzylideneamino)-2-phenylquinazoline-4(3H)-ones by synthesising Schiff-bases from 3-amino-2-phenyl quinazoline-4(3) H-one with different compounds with substituted carbonyl (scheme 3). The developed compounds cytotoxicity and antiviral activity were tested on herpes simplex virus-2 (G), vesicular stomatitis virus, para influenza-3 virus, Sindbis virus, Punta Toro virus, influenza A H1N1 subtype, feline herpes virus, influenza B virus, influenza A H3N2 subtype, feline corona virus (FIPV), respiratory syncytial virus, Coxsackie virus B4, para influenza-3 virus, vesicular stomatitis virus and herpes simplex virus-1

(KOS), herpes simplex virus-2 (G). Against all the tested viruses, compound 2A displayed the best antiviral activity.[22]

Table 2. R and R_1 groups in the Schiff-base compounds developed by Kumar *et al*.[22]

Compound	R	R_1
2A	H	2-OH
2B	H	3-NO_2
2C	H	4-OCH_3
2D	H	4-$N(CH_3)_2$
2E	CH_3	4-Cl
2F	H	H
2G	H	4-OH
2H	CH_3	H
2I	CH_3	4-OH
2J	H	4-Cl
2K	H	3-OH & 4-OCH_3
2L	H	2-OCH_3

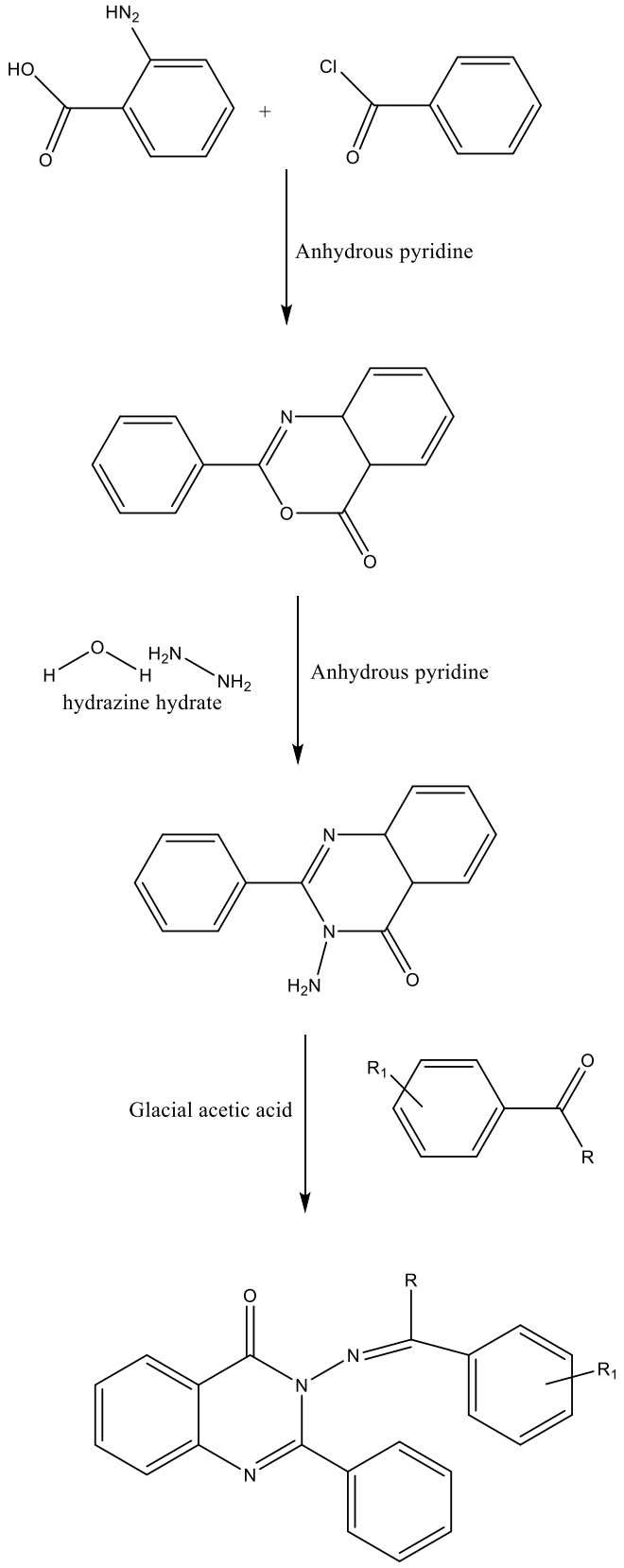

Scheme 3. Schiff-base compounds developed by Kumar *et al.*[22]

1.3.5 Anticancer Schiff base complexes

Malignant neoplasm or what is better known as cancer is a condition where cells of a certain part of the body show growth and reproduce in an uncontrolled way. Invasion to the surrounding normal tissue and metastasis can occur.[23, 24] As the second leading cause of death among humans right after cardiovascular illnesses, it poses a genuine public health issue through the entire world.[25] Nowadays, surgical removal of tumours and chemotherapy are the main ways of treating cancer patients. However, the currently used chemotherapy medications have many side effects and are not effective enough. Schiff-base complexes have been developed lately which showed some anticancer characteristics.[3]

In 2012, Zhang *et al.*, developed three Schiff-base metal complexes (figure 13) derived from the same Schiff-base ligand. They used copper, zinc and cadmium metals to synthesis the aforementioned Schiff-base complexes. All complexes were tested against breast cancer cells of the type MDA-MB-231. Cellular proliferation was inhibited by all three complexes. However, the cadmium complex showed the highest cellular proliferation inhibition and have the ability to trigger apoptosis of the tested cells.[26]

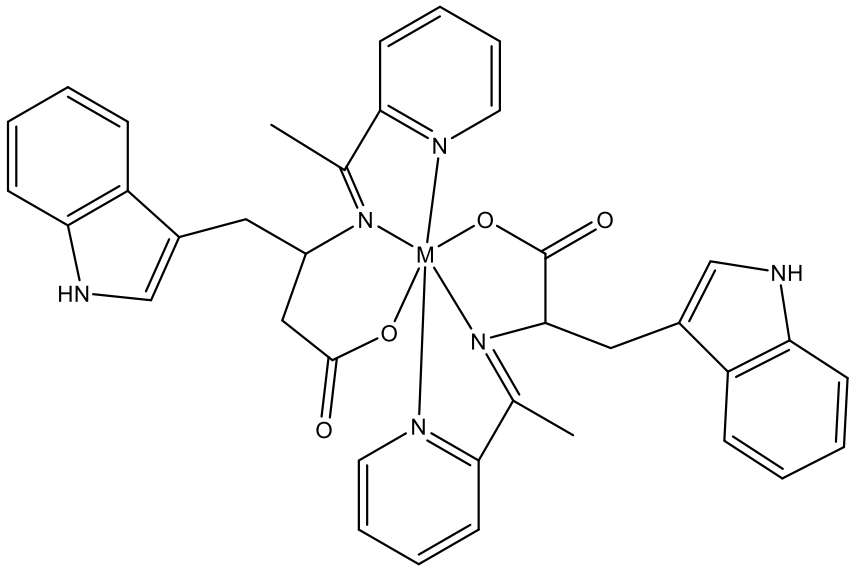

Figure 13. Schiff-base complexes developed by Zhang *et al*.

2012. M= Copper, zinc or cadmium.[26]

In 2013, Li *et al.*, developed water soluble platinum Schiff-base complexes (figure 14). These complexes were tested as anticancer agents towards BGC-823, Bel-7402, KB and HL-60 cell lines. Complex g showed an enhanced cytotoxicity towards BGC-823 and HL-60 and close cytotoxicity towards Bel-7402 compared to cisplatin.[27]

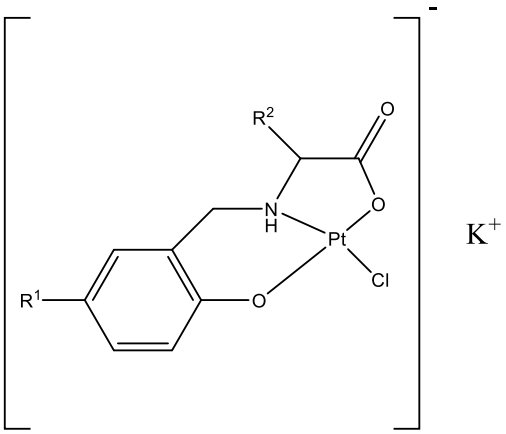

Figure 14. Platinum Schiff-base complexes developed by Li *et at*. 2013

a: R^1=H, R^2=H. b: R^1=H, R^2=benzyl. c: R^1=H, R^2=CH_2OH. d: R^1=H, R^2=Bu^i.

e: R^1=H, R^2=$CH(OH)CH_3$. f: R^1=Br, R^2=CH_2OH. g: R^1=Br, R^2=Bu^i. h: R^1=Br, R^2=H. [27]

In 2014, Hajrezaie *et al.*, reported a copper(II) Schiff-base complex that have a potent antiproliferative influence on HT-29 colon cancer cell line. The study found that cooper(II) complex (figure 15) caused elevation of the reactive oxygen species (ROS) and no significant elevation of caspase 8 at 6.25 µg/ml concentration. The results show that the copper complex can be further studied in order to develop new chemotherapy agents.[28]

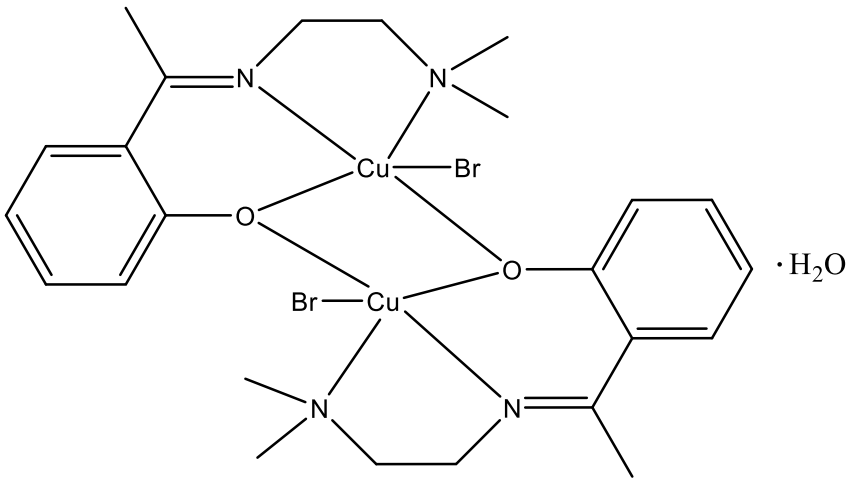

Figure 15. The copper(II) complex by Hajrezaie *et al*. 2014.[28]

1.4 Schiff bases complexes as medical imaging agents

One of the most important medical imaging options is the quantitative emission tomography. There are two main modalities in this field: single photon emission computed tomography (SPECT) and positron emission tomography (PET). Each has its own advantages and disadvantages. PET has very high sensitivity and spatial resolution than SPECT. On the other hand, SPECT radiotracers have longer biological half-lives and are readily available with no need to be located very close to the producing medical cyclotron.[29]

Single photon emission computed tomography (SPECT) relies on the detection of photons produced by the decay of the unstable atom of the used radiotracer. From the areas of radiopharmaceutical uptake, the photons are emitted. Those photons might interact with matter depending on the depth they emitted from. Physical collimation is necessary to overcome issues that might arise from those possible interactions. For this reason SPECT is considered to have lower sensitivity and spatial resolution.[30] SPECT clinical applications include: functional lung scanning, myocardial perfusion imaging and bone scanning by ^{99m}Tc.[31, 32]

Positron emission tomography (PET), a technology that emerged in 1970's [33], is a medical imaging modality based on the basic principal of detecting two high energy photons at the same time on 180 degrees from each other emitted from the annihilation of the positron, emitted from a positron emitting radioisotope, as it combine an electron from surrounding atoms.[30] It is widely used in the fields of oncology, cardiovascular and neurological

imaging.[34] Comprehensive research in different applications of PET led to the clinical use in those fields. In the field of oncology, PET nowadays is used for neoplasm detection and differentiation between malignant and benign tumours, tumour staging, treatment evaluation, radiotherapy planning and the developing new anti-cancer drugs.[35]

In 1996, Marmion *et al.*, developed sixteen N_3O_3 Schiff-base ligands (figures 16 and 17 and table 3) which can encapsulate ^{99m}Tc (IV) ions in order to make new ^{99m}Tc radiopharmaceuticals. Metabolism studies reported a myocardial uptake up to 2% of the dose injected.[36]

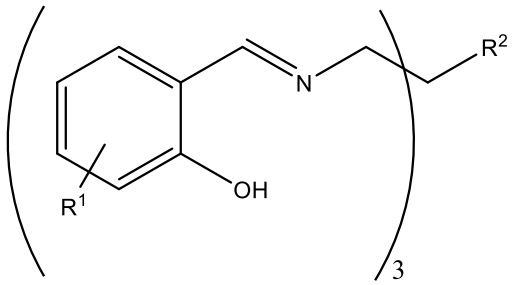

Figure 16. **1-9**, **14-16** Schiff-base ligands developed by Marmion *et al*. 1996.[36]

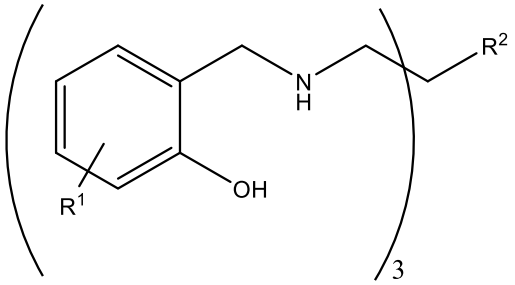

Figure 17. **10-13** Schiff-base ligands developed by Marmion *et al*. 1996.[36]

Table 3. R^1 and R^2 groups in the Schiff-base compounds developed by Marmion *et al*. 1996.[36]

Compound	R	R_1
1	H	CH_3
2	5-CH_3	CH_3
3	5-CH_2CH_3	CH_3
4	5-F	CH_3
5	4-OCH_3	CH_3
6	H	CH_2OCH_3
7	H	$CH_2O(CH_2)_2CH_3$
8	H	$CH_2O(CH_2)_5CH_3$
9	H	$CH_2OCH_2(C_6H_5)$
10	5-CH_3	CH_3
11	4-OCH_3	CH_3
12	H	$CH_2O(CH_2)_2CH_3$
13	H	$CH_2OCH_2(C_6H_5)$
14	4-$OCH_2COOCH_2CH_3$	CH_3
15	4-$OCH_2COOC(CH_3)_3$	CH_2OCH_3
16	5-COOH	CH_3

In 2015, Lange *et al.*, reported synthesising new gallium(III) Schiff-base complex (Figure 18). The complex can cross the blood-brain barrier and binds to the Aβ plaques associated with Alzheimer's disease. They suggested the possibility of developing a positron-emitting gallium-68 Schiff-base complex.[37]

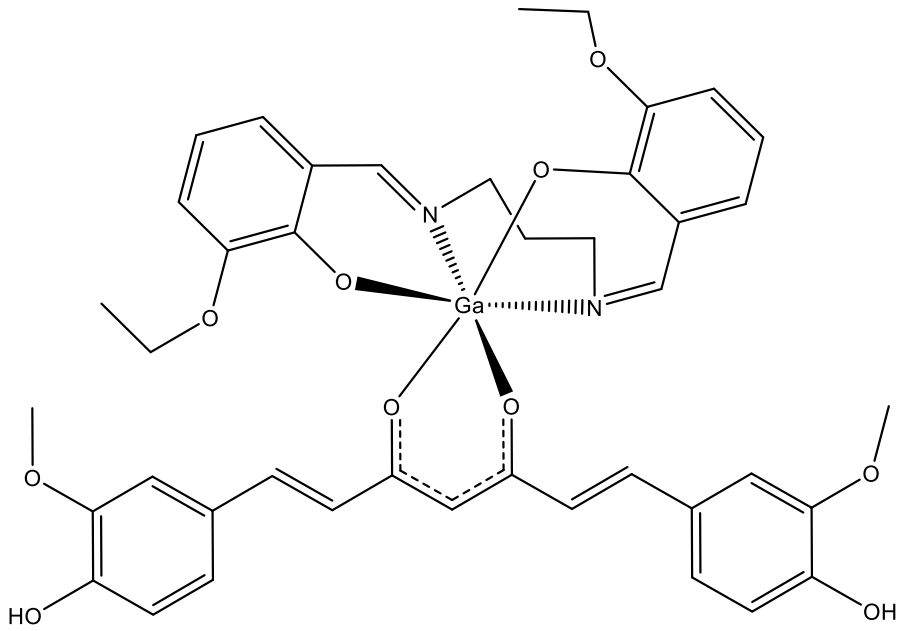

Figure 18. The gallium(III) Schiff-base complex.[37]

1.5 Ligands of interest to this project

1.5.1 Phenoxy-imine Schiff-base ligands

Schiff-base ligands produced by reacting aromatic or aliphatic amines with aromatic aldehydes have been studied extensively.[38] Having two functional groups close to each other constitute as an advantage property of this class of Schiff-base compounds, especially when chelating metal ions.[5]

In 2001, Figuet, developed a number of Schiff-base metal complexes. The aim of their study was to develop new SPECT imaging agent precursor. Gallium(III), indium(III) and thallium(III) metals were used to create the novel Schiff-base complexes (figure 19). The metal ions were bonded to the ligand in the same way by N_3O_3 donor set. This means that their Schiff-base ligand (figure 20) is great for coordinating lanthanide and group 13 metal ions.[39]

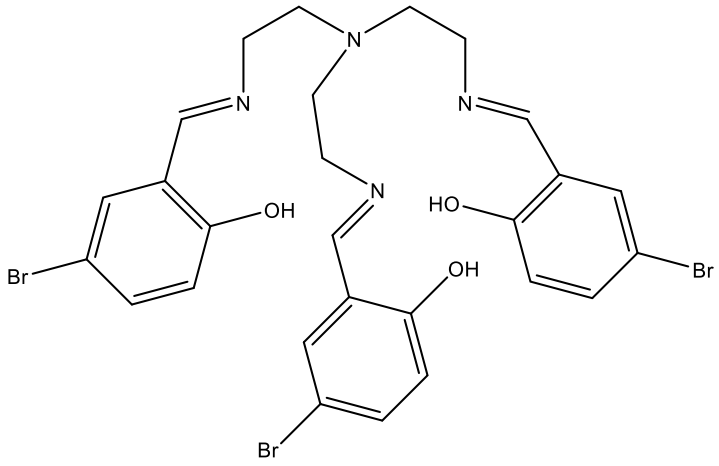

Figure 19. Schiff-base ligand developed by Figuet, in 2001.[39]

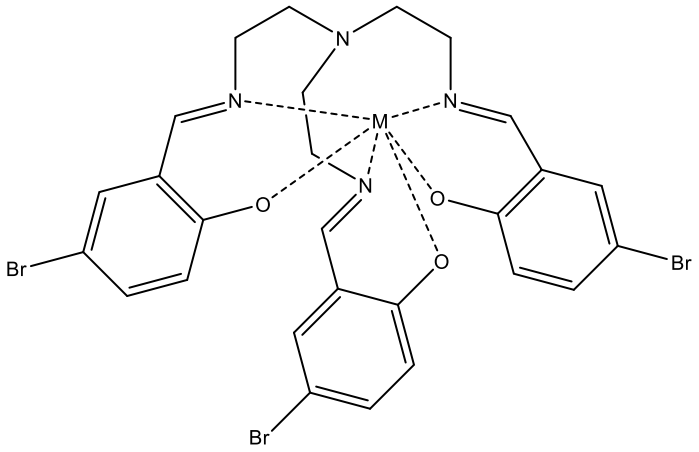

Figure 20. Schiff-base metal complexes developed by Figuet, in 2001.

M= Ga^{III}, In^{III} or Tl^{III}.[39]

In 2005, Khandar *et al.*, synthesized two Schiff-base ligands (scheme 4) and their copper(II) and nickel(II) derivatives. Ligand L_1 acted as a tetradentate and L_2 behaved as a hexadentate ligands. The study concluded that lengthening the alkyl link might cause coordination geometry distortion from square-planer into octahedral.[40]

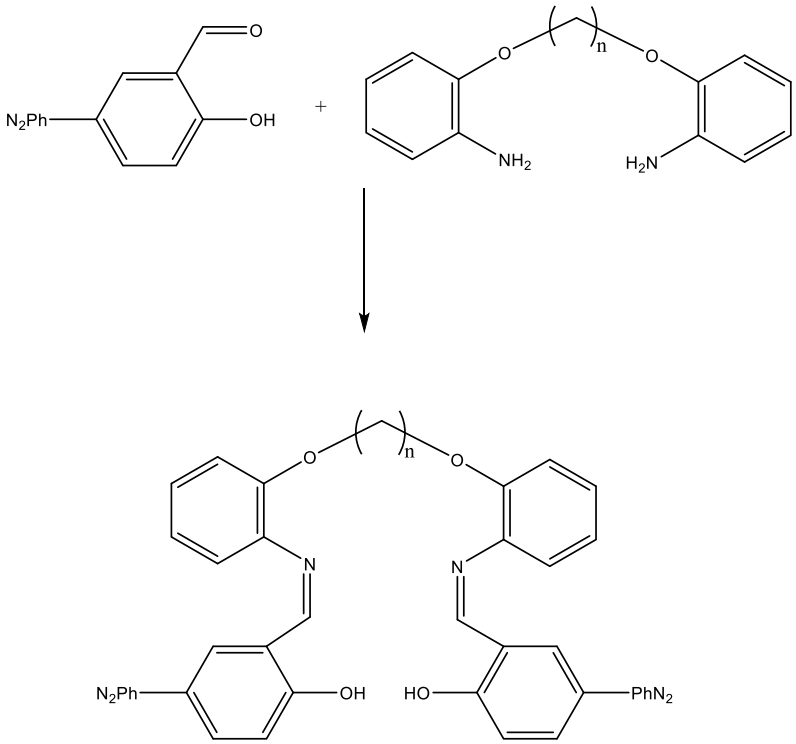

Scheme 4. Synthesis of L_1 and L_2 ligands prepared by Khandar *et al*. in 2005.[40]

L_1 n=2, L_2 n=4

In 2015, Hossain *et al.*, synthesized a Schiff-base ligand (scheme 5) from condensation of 2-picolyl amine with 1,1-bis-[2-hydroxy-3-acetyl-5-methylphenyl]methane. The ligand was tested to determine its ability of serving as a “Turn-On” fluorescence chemosensor for aluminium^{3+}. The study concluded that the ligand has the potential to work as detection sensor for aluminium^{3+}.[41]

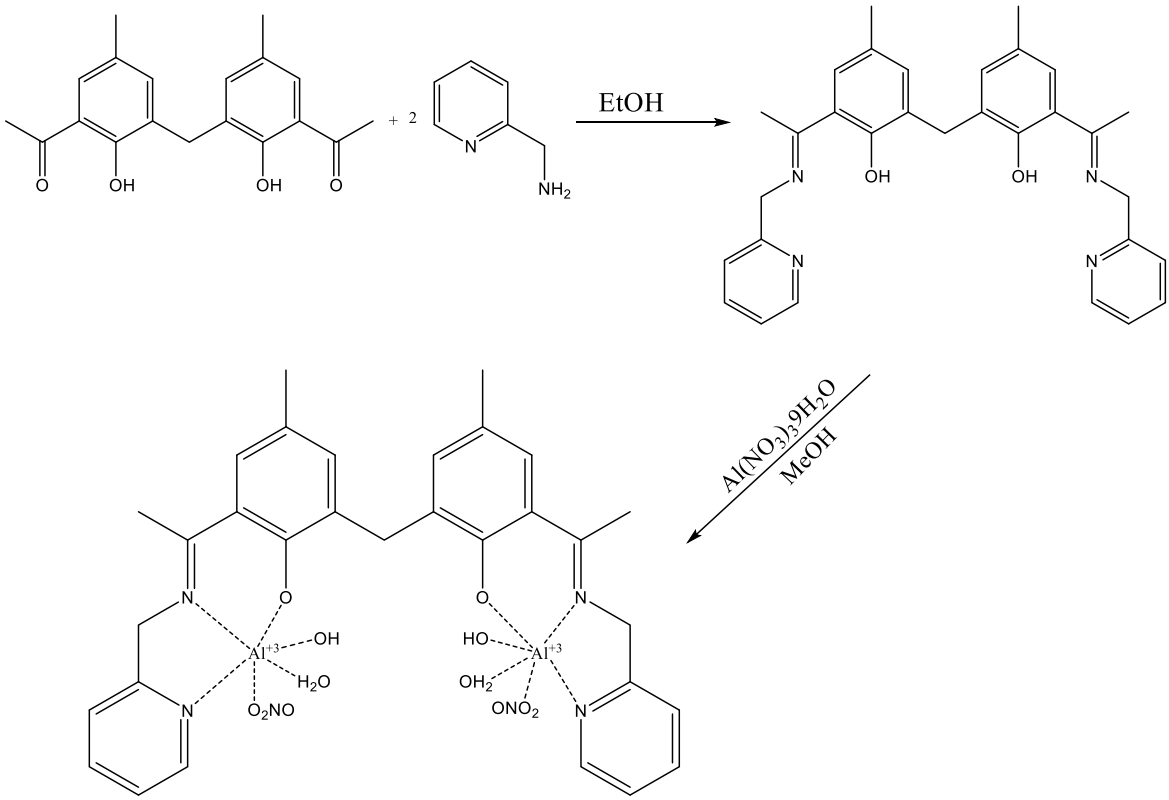

Scheme 5. The Schiff-base ligand developed by Hossain *et al*. in 2015.[41]

1.5.2 Macrocyclic Schiff base ligands

Macrocyclic ligands have the advantage of forming highly stable complexes.[2] The biomedical oriented research into macrocycles developed in the 80's and 90's of the past century and expanded since the start of the 21st century.[14, 15] Over the years, numerous Schiff-base macrocyclic complexes have developed for biomedical applications.[42] In addition to their pharmacological properties, the capacity of Schiff-bases for chemical recognition of metals and anions and their coordination behaviour and soft-hard donor character are appealing properties that led to popularity of macrocyclic Schiff-base ligands.[43-48]

In 2005, Raman *et al.*, reported making a new Schiff-base macrocyclic ligand (figure 21) and its copper, nickel, cobalt and zinc derivatives. The ligand and the complexes antimicrobial activity was assessed in vitro using well-diffusion method towards Gram-negative bacteria Escherichia coli and Salmonella typhi and Gram-positive bacteria Staphylococcus aureus, viz. Klebsiella pneumonia and Bacillus subtilis. The study concluded that the complexes showed higher activity than the free Schiff-base ligand. The strength of the complexes activities varied against each bacteria strain. In the case of Staphylococcus aureus cobalt was the strongest then zinc > copper > nickel and last was the free ligand. For Klebsiella pneumonia, also cobalt was the strongest followed by copper and nickel at the same strength, then zinc was stronger than the free ligand. For Bacillus subtilis, copper showed the highest activity followed by zinc > nickel > cobalt and the free ligand showed the least activity. For the Escherichia coli, cobalt > zinc >

nickel > copper > free ligand. For Salmonella typhi, zinc > copper > cobalt > nickel > free ligand.[49]

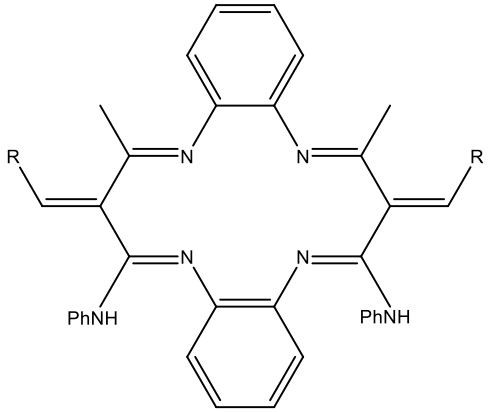

Figure 21. The Schiff-base macrocyclic ligand developed by Raman *et al*. in 2005.[49]

In 2010, Singh *et al.*, reported synthesising and characterizing of new macrocyclic Schiff-base chromium(III), iron(III) and manganese(III) complexes (scheme 6). The complexes were tested against A. fumigatus and Aspergillus niger fungal strains for their in vitro antifungal activities. The $[Cr(C_{28}H_{24}N_4)Cl]Cl_2$ complex showed the highest antifungal activity.[50]

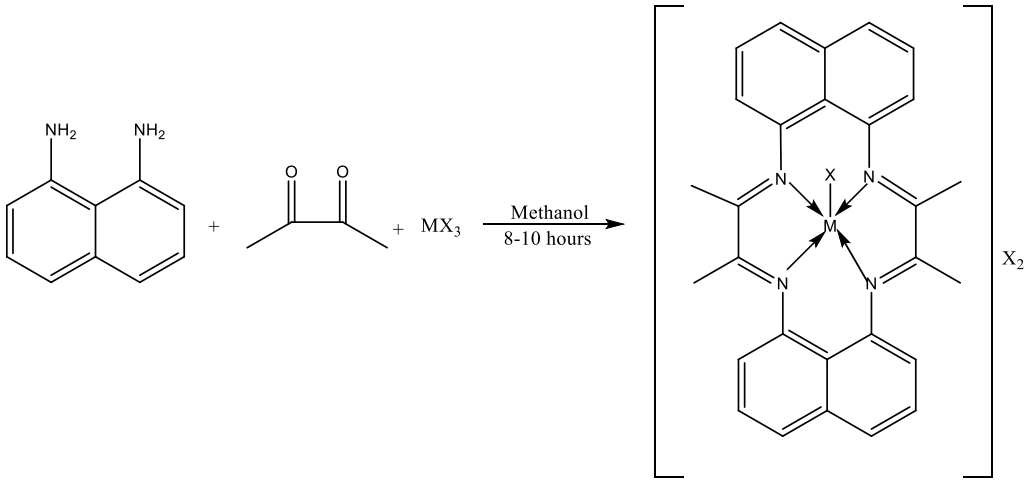

Scheme 6. The Schiff-base macrocyclic complexes developed by Singh *at al.* in 2010.[50]

M= Cr(III), Fe(III) or Mn(III). X= Cl^-, NO_3^- or CH_3COO^-.

Novel copper(II) and manganese(II) Schiff-base macrocyclic complexes (scheme 7) were developed and characterized by Kumar *et al.* in 2010. The complexes antifungal activities were tested towards F. odum, A. alternate, F. oxysporum and A. niger fungi strains. They concluded that the complexes showed good antifungal activities.[51]

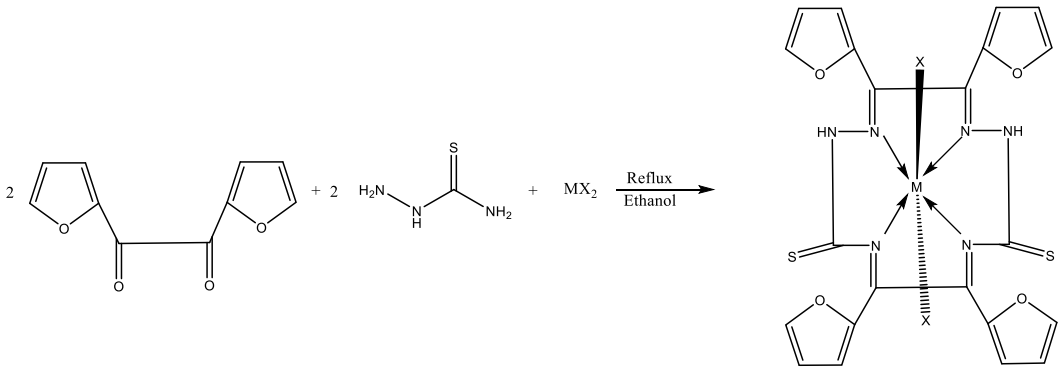

Scheme 7. The Schiff-base macrocyclic complexes developed by Kumar *et al*. in 2010.[51]

M= Cu(II) or Mn(II). X= Cl^-, NO_3^- or NCS^-.

In 2011, Pawar *et al.*, reported the synthesis of two Schiff-base macrocyclic ligands and their oxovanadium complexes (figures 22 and 23). The macrocyclic Schiff-base ligands and oxovanadium complexes were tested in vitro for their antibacterial activities on Bacillus licheniformis, Micrococcus luteus, Staphylococcus aureus and Escherichia coli bacteria strains. The oxovanadium complexes showed more antibacterial activity than its precursor ligands. The antibacterial activity increased with increasing concentrations. The macrocyclic Schiff-base ligands and their oxovanadium complexes also showed varying antioxidant activities compared to ascorbic acid.[52]

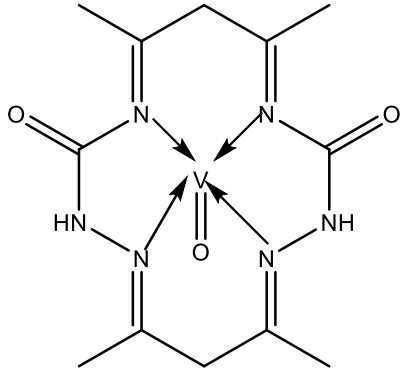

Figure 22. The first oxovanadium Schiff-base complex Pawar *et al*. made in 2011.[52]

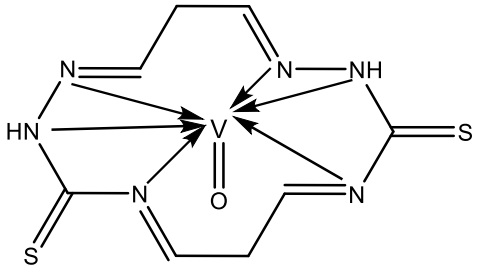

Figure 23. The second oxovanadium Schiff-base complex Pawar e*t al*. made in 2011.[52]

In 2013, Shiekh *et al.*, synthesized novel mixed thia-aza-oxo Schiff-base macrocycle and its cobalt(II), copper(II), nickel(II), and manganese(II) derivative complexes (scheme 8). The complexes showed metal centred reduction when tested by cyclic voltammetry. In addition, both copper(II) complexes exhibited reduction and oxidation process. In vitro tests of the ligands and its metal complexes on Candida albicans, Candida tropicalis, Candida glabrata and Candida kruesi. The results showed that the metal complexes exhibited an elevated inhibitory effect than the Schiff-base macrocyclic free ligand.[53]

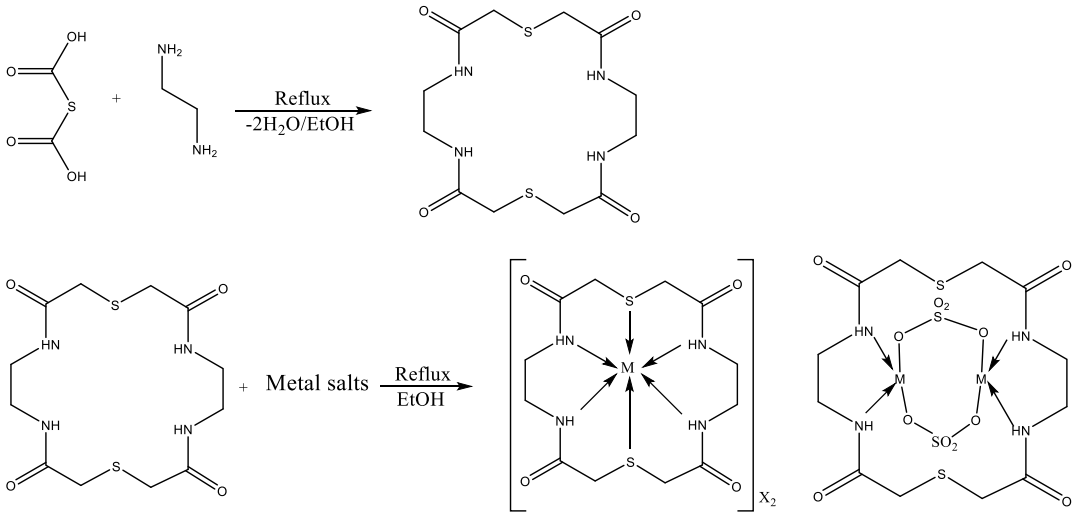

Scheme 8. The Schiff-base macrocyclic ligand and metal complexes made by Shiekh *et al*. in 2013.[53]

M= Co(II), Cu (II), Mn(II) or Ni(II). X=Cl^- or NO_3^-.

In 2013, Ahmed *et al.*, reported synthesising of a novel Schiff-base macrocyclic ligand and its cobalt(II), manganese(II), nickel (II), zinc(II), and copper(II) derivatives (scheme 9). The macrocyclic Schiff-base ligand and its metal derivative complexes were tested for their biological activities against Escherichia coli, Staphylococcus aureus bacteria strains and the results showed higher antimicrobial activity of the metallic complexes in comparison to the free ligand. On the other hand, the Schiff-base ligand and its metal derivatives had no effect on Pseudomonas aeruginosa bacteria strain.[54]

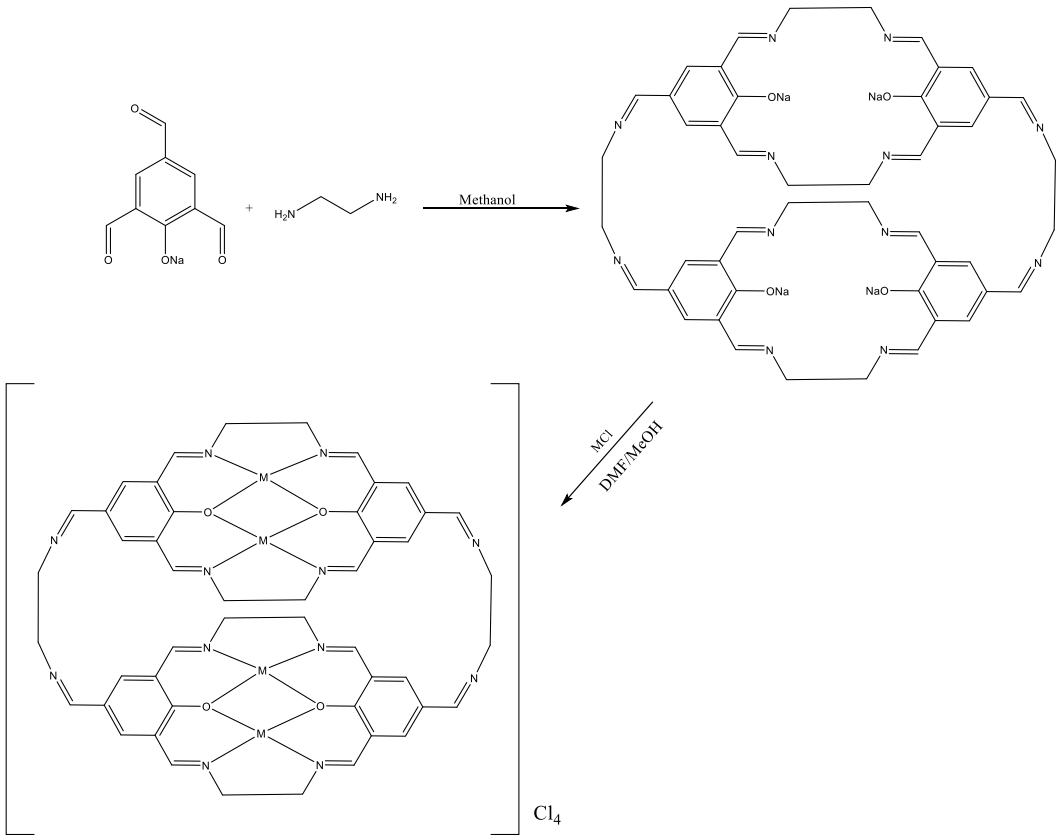

Scheme 9. The macrocyclic Schiff-base ligand and its metal derivatives reported in 2013 by Ahmed *et al*.[54]

M= Co(II), Mn(II), Cu(II), Ni(II) or Zn(II).

In 2015, Gull and Hashmi reported the synthesis and characterisation of a novel Schiff-base macrocyclic ligand and its cobalt(II), copper(II) and nickel(II) metal complexes (scheme 10). The Schiff-base macrocyclic ligand and its metal derivatives were tested in vitro towards Bacillus subtilis, Escherichia coli, Staphylococcus aureus and Pseudomonas aeruginosa bacteria strains, and Fusarium sp, Trichosporon sp, Aspergillus flavus and Candida albicans fungal species. The metal complexes exhibited greater antibacterial and antifungal activities than the macrocyclic Schiff-base free ligand.[55]

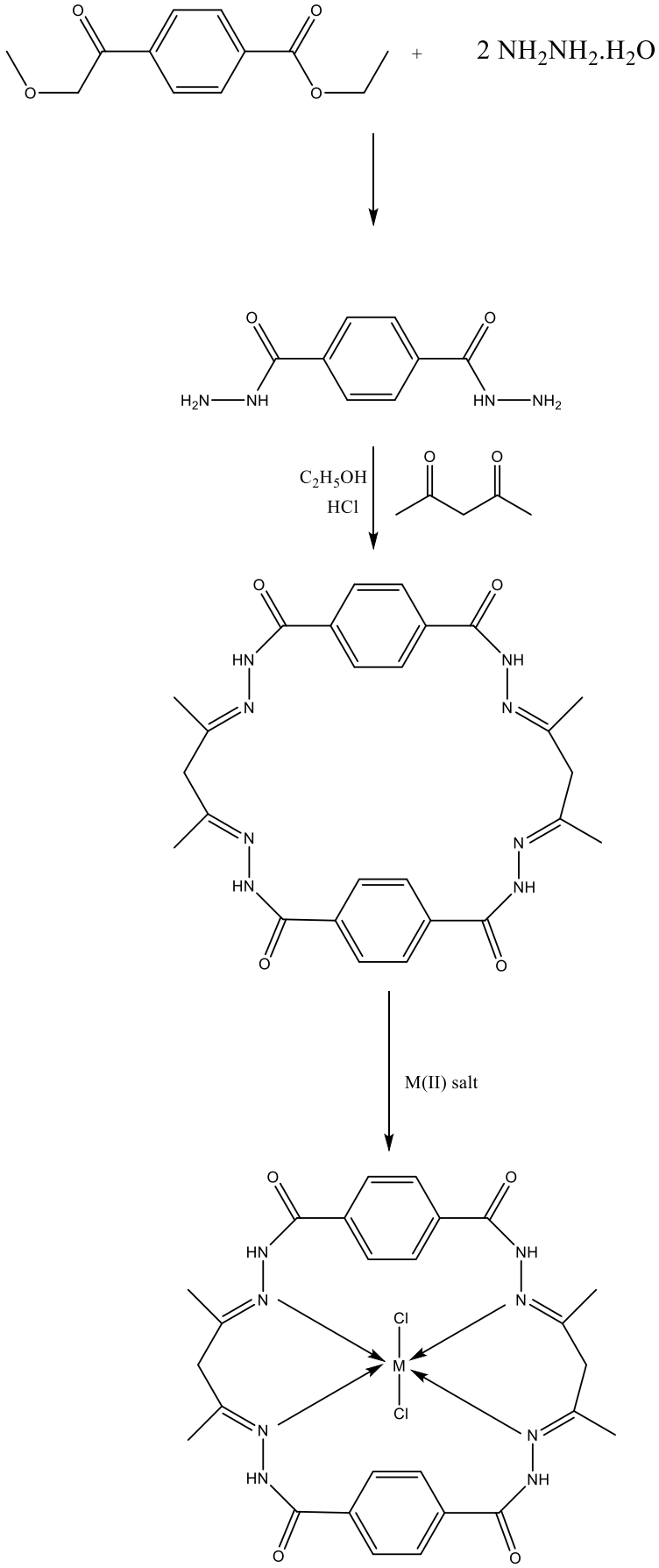

Scheme 10. The macrocyclic Schiff-base ligand and its metal complexes prepared by Gull and Hashmi in 2015.[55]

M= Cu(II), Co(II) and Ni(II)

1.6 Copper:

Copper is a transitional metal with two main oxidation states, +1 and +2. It comes after zinc and iron as most abundant trace elements in the human body, which makes it a vital to life. However, if 80,000µg to 100,000µg is ingested by human, it becomes toxic.[56-60] Copper displays noticeable biochemical activities as a part of many externally administrated chemical compounds or as a vital trace metal in the human body.[61] Current research around copper complexes focused on its anti-inflammatory, antimicrobial, antiviral and anticancer potential.[62]

Coordination chemistry of the aqueous solution of copper is restricted to oxidation states I, II and III.[63-65] Copper(I) complexes do not have adequate kinetic stability required for radiopharmaceutical applications and copper(II) is not easy to obtain without using strong π-donating ligands. On the other hand, copper(II) is considered a d^9 metal that favours bidentate, imines and amine ligands in order to form square pyramidal, trigonal pyramidal, square planar, distorted square planar and distorted octahedral geometries.[66]

Furthermore, there has been significant research around copper radionuclides (table 4). The will defined coordination chemistry of copper permit connecting it with various chelating systems which in turn can be connected to proteins, antibodies, peptides and other biologically important molecules. Due to its longer half-life and the fact that it can be delivered to nuclear medicine departments with approximately one half-life lost during the process, copper 64 has been the main focus of researchers in this field. Additionally, copper 64 half-life is consistent with time frames necessary for

ideal bio-distribution of slower clearing agents including nanoparticles and monoclonal antibodies (mAbs) which needs longer imaging times.[66]

Table 4. Copper radionuclides.[66]

Isotope	Half life	β^- MeV %	β^+ MeV %	EC %	γ MeV
^{60}Cu	23.4 minutes	_____	2.00 (69) 3.00 (18) 3.92 (6)	7.0	0.511 (186) 0.85 (15) 1.33 (80) 1.76 (52) 2.13 (6)
^{61}Cu	3.32 hours	_____	1.22 (60)	40	0.284 (12) 0.38 (3) 0.511 (120)
^{62}Cu	9.76 minutes	_____	2.91 (97)	2	0.511 (194)
^{64}Cu	12.7 hours	0.573 (38.4)	0.655 (17.8)	43.8	0.184 (40) 1.35 (0.6)
^{67}Cu	62.0 hours	0.395 (45) 0.484 (35) 0.577 (20)	_____	_____	0.184 (40)

Tetraazamacrocyclic ligands are the most widely used chelators for connecting copper 64 with antibodies, proteins and peptides. They have pendant arms that employ chelate and macrocyclic effects to improve the molecule stability. DOTA (1,4,7,10-tetraazacyclododecane-1,4,7,10-tetraacetic acid) (figure 24) and TETA (1,4,8,11-tetraazacyclotetradecane-1,4,8,11-tetraacetic acid) (figure 25) are the most extensively studied chelators for copper 64. Due to DOTA's low stability and capacity to bind different metals, it is not ideal for chelating copper 64.[166-171] Therefore,

TETA has been widely utilized as copper 64 chelator with successful derivatization of TETA that led researchers to attach it to biologic molecules.[172-179] However, when ^{64}Cu-TETA complex is used *in vivo*, 20 hours after injection approximately 70% of the copper 64 tranchelate to a 35-kDa species presumed to be superoxide dismutase (SOD) in the liver.[67]

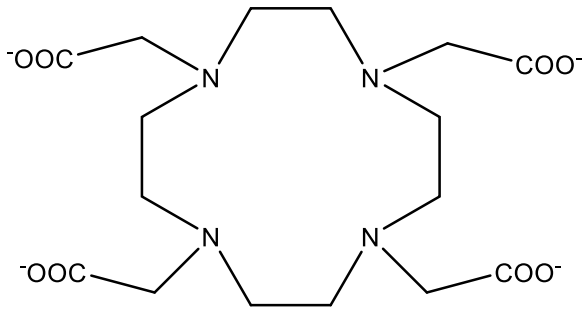

Figure 24. DOTA ligand.[67]

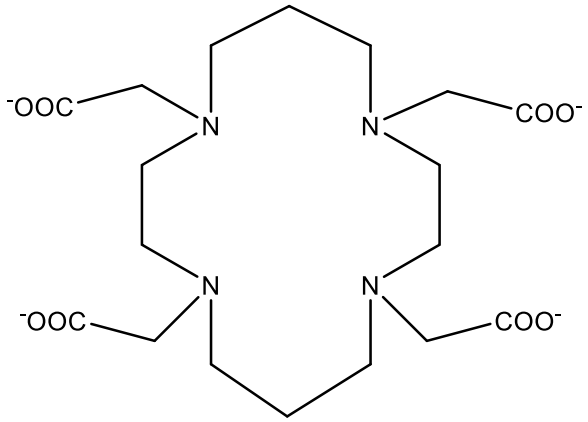

Figure 25. TETA ligand.[67]

Fujibayashi *et al.* discovered back in 1997 that diacetyl-2,3-bis(N4-methyl-3-thiosemicarbazone) copper complex known as Cu-ATSM (figure 26), exhibited hypoxia uptake in - perfused, ischemic, isolated rat heart models.[68, 69] Prior to routine clinical use of radiolabelled Cu-ATSM, estimated human dose was calculated to be between 500 and 800 MBq.[70] Lewis *et al.*, reported in 2008 a clinical comparison between ^{60}Cu-ATSM and ^{64}Cu-ATSM imaging properties in uterine cervix cancer. The study

results showed that Cu-ATSM is an indicator for chronic tumour hypoxia.[71, 72]

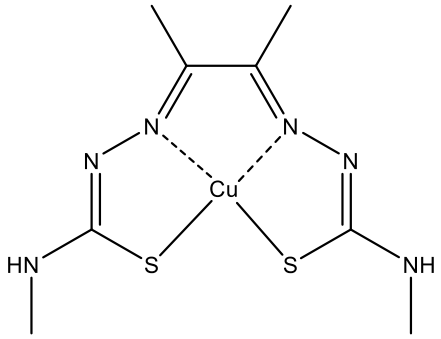

Figure 26. Cu-ATSM complex.[68, 69]

In 2007, Pressly *et al.*, reported preparing amphiphilic copolymers with prearranged reactive functionalities and polyethylene glycol (PEG) chains that have different length and low polydispersity. The aim was to label these nanoparticles with copper 64 using DOTA chelator. The study concluded that the longer the PEG chain in the particle the longer it circulate in the blood and the lower it concentrate in the liver.[73, 74]

The table (table 5) below contain the most notable copper phenoxy-imine compounds and their route of synthesis found on the Cambridge crystallography data centre website:

Table 5. Most notable copper phenoxy-imine compounds and their route of synthesis found on the Cambridge crystallography data centre website.

	Copper phenoxy-imine complex	**Route of synthesis**
1	Figure 27 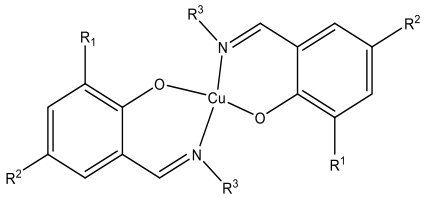 **L1:** R^1=R^2=Me, R^3=(4-MeO)C_6H_4 **L2:** R^1=*t*-Bu, R^2=Me, R^3=(4-MeO)C_6H_4 **L3:** R^1=R^2=Br, R^3=(2,6-*i*-Pr_2)C_6H_4 **L4:** R^1=*t*-Bu, R^2=Me, R^3=(4-MeO)$C_6H_4CH_2$	1.0mmol of Schiff-base in 20.0cm^3 of methanol added to 0.5mmol of copper acetate in 10cm^3 of methanol. The mixture is refluxed for 2 hours. After cooling to room temperature, methanol is removed under reduced pressure, and dry residue is recrystallized from dichloromethane.[75]

2	Figure 28 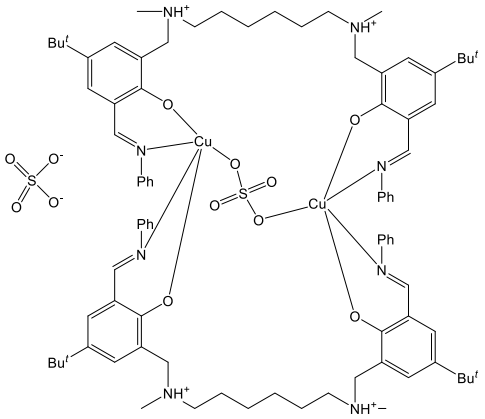	Equal amounts of the Schiff-base ligand and copper sulphate refluxed in methanol for 2 hours. The mixture was filtered while hot then concentrated to about 30% of its original volume and left standing at room temperature. Crystals were collected, washed with cold ethyl acetate then with ether and dried under reduced pressure.[76]
3	Figure 29 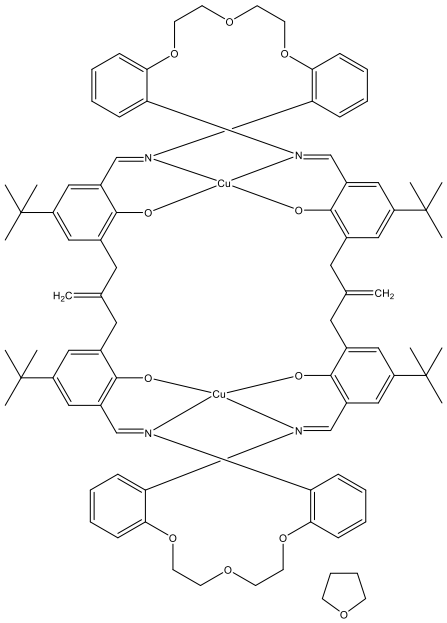	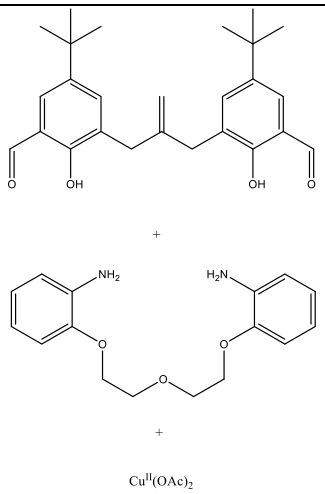 Figures 30. Ligands L1 and L2. 0.5mmol of L1 and L2 in 10.0ml of THF. Dark brown crystals was obtained in THF.[77]
4	Figure 31 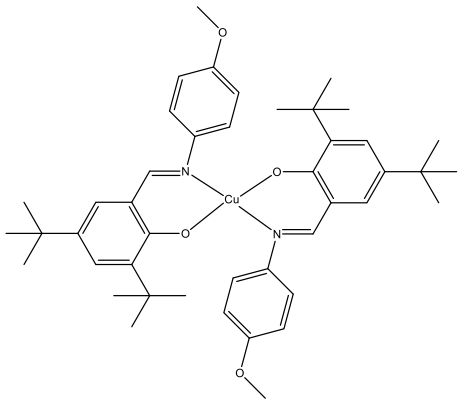	0.5mmol of copper (II) perchlorate in 10.0ml methanol was added to 1.0mmol of 2-((4-methoxyphenylimino)methyl)-4,6-di-*tert*-butylphenol in 10.0ml of methanol, then 1.0mmol of Et_3N was added to the mixture. It was stirred in room temperature for 5 hours then the precipitated solid was isolated by filtration and dried in air. Crystallization was done using dichloromethane and methanol solution.[78]

5	Figure 32 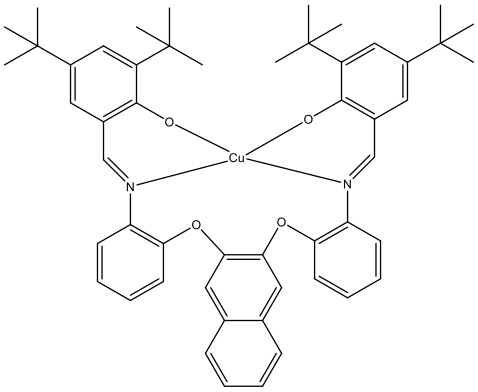	(0.37g, 1mmol) of $Cu(ClO_4)_2.6(H_2O)$ in 15.00ml of methanol and excess NEt_3 is added to a warm methanol solution (50.00ml) of 6,6'-((1E,1'E)-(((naphthalene-2,3-diylbis(oxy))bis(2,1-phenylene))bis(azaneylylidene))bis(methaneylylidene))bis(2,4-di-*tert*-butylphenol) Schiff-base. For 4 hours the mixture was refluxed, and the resulting green solid is collected via filtration and washed with cold methanol. Liquid diffusion of acetonitrile into a toluene solution of the complex afforded green crystals.[79]
6	Figure 33 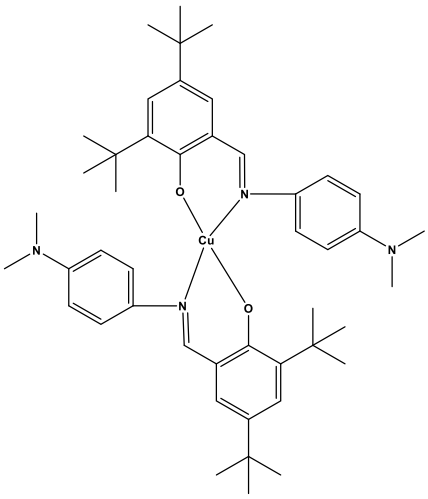	(705mg, 2mmol) of N-(4-dimethylaminophenyl)-3,5-di-*tert*-butylsalicylaldimine in 20ml of hot methanol added to (200mg, 1mmol) of $Cu(OAc)_2{\cdot}H_2O$ in 20ml of hot methanol and refluxed for 4 hours. Then, the volume was reduced to 50% of its original volume and cooled to 20°C. the resulting brown precipitate was filtered and washed with methanol and recrystallized using dichloromethane and methanol solution.[80]
7	Figure 34 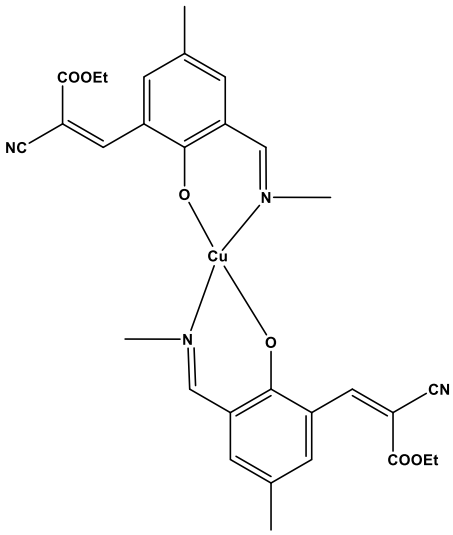	(45.00mg, 0.12mmol) of $Cu(ClO_4)_2.6H_2O$ in 5.0ml of methanol added to (84.00mg, 0.24mmol) of ethyl 2-cyano-3-(2-hydroxy-5-methyl-3-(ptolylimino)methyl)phenyl)acrylate and stirred for 2 hours. The precipitated dark brown solid was filtered and washed with ether and hexane. Recrystallization was done with a hexane and dichloromethane solvent mixture.[81]

8	Figure 35 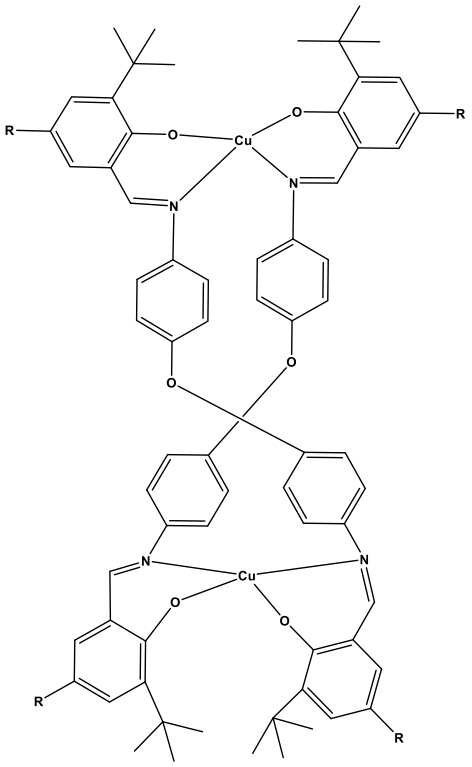 R= Me or *t*-Bu.	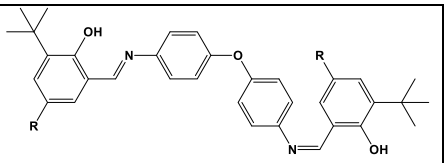 Figure 36. Schiff-base ligand 1 (R=Me) and ligand 2 (R=t-Bu). (0.32g, 0.50mmol) of ligand 1 or (0.27g, 0.50mmol) of ligand 2 in 25.00ml of methanol added to (0.19g, 0.50mmol) of $Cu(ClO_4)_2 \cdot 6H_2O$ in 25.00ml of methanol which turned the solution into brown immediately. The mixture was refluxed for 2 hours then cooled to room temperature and filtered. The filtrate was left to evaporate slowly to give brown crystals.[82]
9	Figure 37 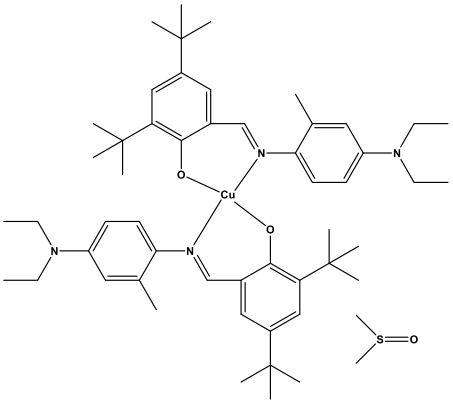	To 2mmol of N-(4-diethylamino-2-methly-phenyl)-3,5-di-*tert*-butylsalicylaldimine in 10ml of DMSO, 1mmol of $Cu(OAc)_2.H_2O$ dissolved in 10ml of DMSO was added. The mixture was refluxed for 10 hours then the DMSO was removed under reduced pressure. Brown solid was then washed with 5 ml of water twice and 5ml of ethanol. The resulting product was filtered and crystalized in dichloromethane (3ml) and ethanol (10ml).[83]

10	Figure 38 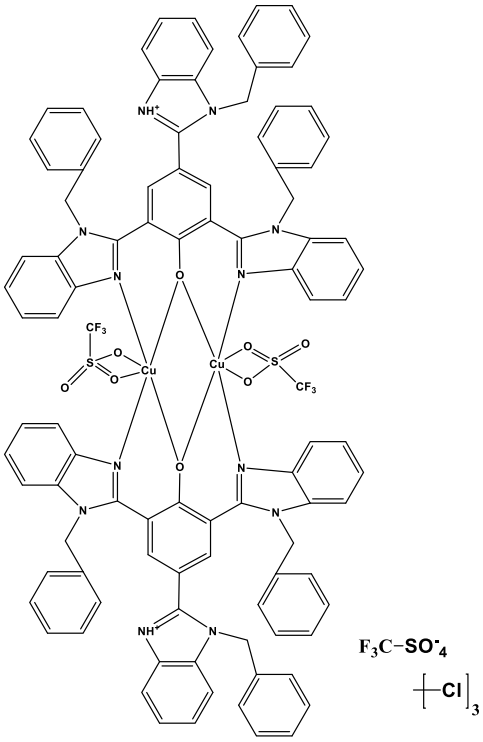	(0.021g, 0.030mmol) of 2,4,6-Tris(1-benzyl-benzimidazol-2-yl)phenol in 5ml of chloroform added to (0.026g, 0.050mmol) of $Cu(MePhSO_3)_2{\cdot}6H_2O$ in 3ml of methanol. The mixture was moved into a test tube which was sealed in a bottle that contains 20ml of diethyl ether. After few days, the diethyl ether was diffused and yellow and green crystals (the desired compound) have formed. Crystals were made from chloroform and acetonitrile mixture upon diffusion of diethyl ether.[84]
11	Figure 39 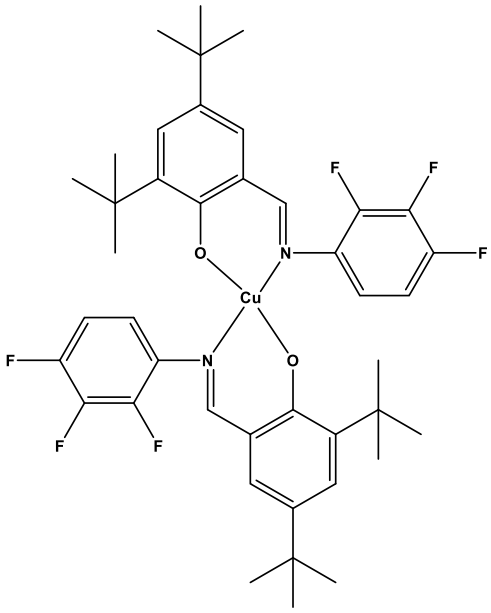	(0.1g, 0.5mmol) of $Cu(OAc)_2.H_2O$ in 5ml of methanol added to (0.36g, 1.00mmol) of N-2,3,4-trifluorophenyl-3,5-di-*tert*-butylsalicylaldimine dissolved in 60ml of hot methanol. The mixture is refluxed for one hour then the volume is reduced to about 30ml and kept in air at room temperature. Green crystals were obtained after one day.[85]

12	Figure 40 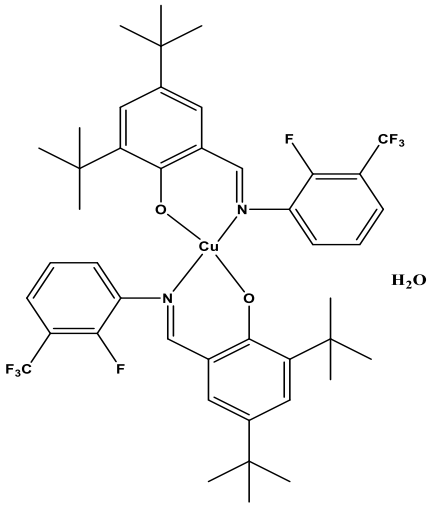	0.5mmol of $Cu(OAc)_2.H_2O$ in 10ml of methanol was added to 1.0mmol of (E)-2,4-di-*tert*-butyl-6-(((2-fluoro-3-(trifluoromethyl)phenyl)imino)methyl)phenol in 50ml of hot methanol. . The mixture is refluxed for one and a half hours then the volume is reduced to about 30ml and left at room temperature. Microcrystals were collected by filtration and washed with clod methanol and dried in air.[86]
13	Figure 41 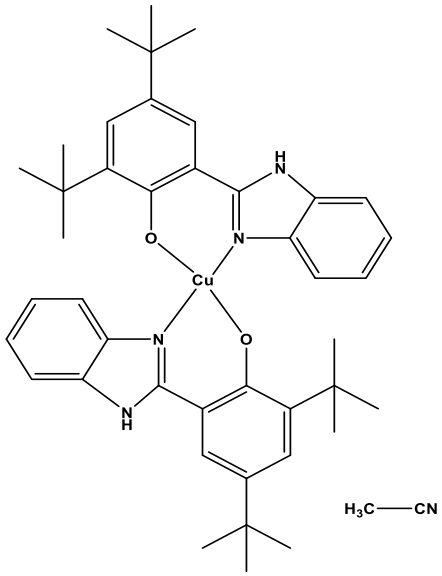	(317.00mg, 1.24mmol) of $Cu(BF_4)_2{\cdot}H_2O$ in 5ml of methanol added to (800.00mg, 2.48mmol) of 2-(1H-benzo[d]imidazol-2-yl)-4,6-di-*tert*-butylphenol in 50ml of methanol. The mixture was stirred at room temperature for about one hour then a few drops of trimethylamine was added and stirring continued for a further hour. The solvent was removed under reduced pressure to obtain dark brown solid which was dissolved in diethyl ether and filtered. Then, the diethyl ether was removed under reduced pressure and brown solid was collected. It was then dissolved in acetonitrile and filtered. The filtrate was allowed to evaporate in air. After 3 to 4 days, brown single crystals suitable for x-ray diffraction was obtained.[87]

14	Figure 42 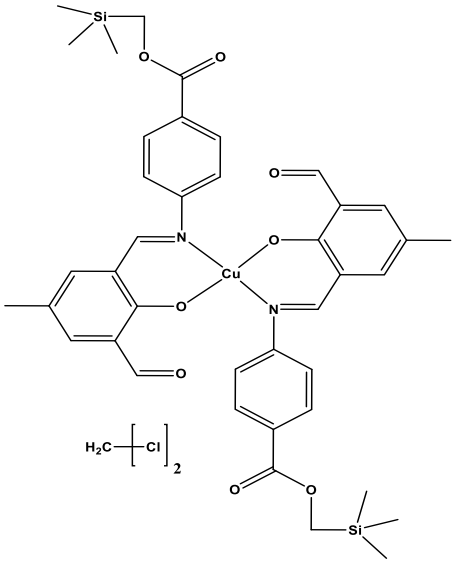	(0.17g, 1.00mmol) of 2,6-diformyl-4-methyphenol in 10ml of a methanol and chloroform solution mixture was added to (0.45g, 2.00mmol) of trimethylsilyl-methyl-p-aminobenzoate in 10ml a methanol and chloroform mixture. It was refluxed for 4 hours then cooled to 50°C and added dropwise to (0.35 g, 2.00mmol) of $CuCl_2{\cdot}2H_2O$ in 5ml of methanol which changed the colour from red to green. The green solution was stirred for 10 minutes and then few drops of trimethylamine were added before stirring again for one hour and filtered. The filtrate was dried under reduced pressure and purified by chromatography.[88]
15	Figure 43 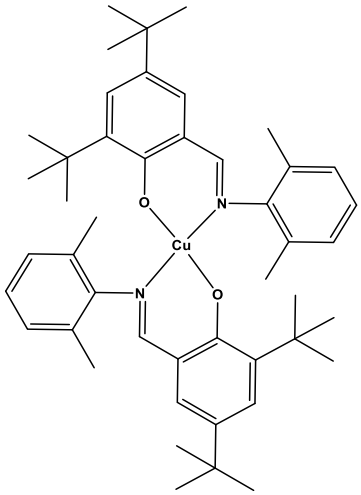	To 0.890mmol of $HOC_6H_2tBu_2C(H)N(C_6H_3Me_2)$ in 10ml of tetrahydrofuran, 0.890mmol of sodium hydride was added. After 30 minutes, 0.445mmol of copper (II) chloride was added. After 12 hours, centrifugation was done to remove the insoluble material and the solvent was removed under reduced pressure. Red crystals were obtained from recrystallization in toluene.[89]

16	Figure 44 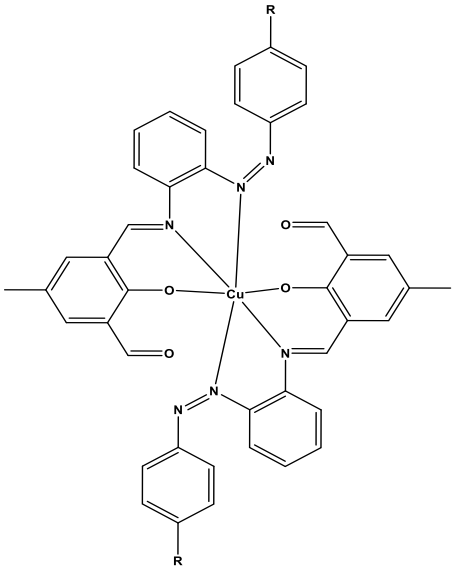 R= H, CH_3 or Cl.	0.29mmol of copper acetate and 0.58mmol of 2-hydroxy-5-methyl-3-((E)-((2-((Z)-phenyldiazenyl)phenyl)imino)methyl)benzaldehye, 2-hydroxy-5-methyl-3-((E)-((2-((Z)-p-tolyldiazenyl)phenyl)imino)methyl)benzaldehyde or 3-((E)-((2-((Z)-(4-chlorophenyl)diazenyl)phenyl)imino)methyl)-2-hydroxy-5-methylbenzaldehyde were stirred in methanol for three hours. Brownish precipitate was filtered off and then dissolved in dichloromethane to form dark brown colour and layered with hexane. After evaporation of the solvent, small crystals were obtained.[90]
17	Figure 45 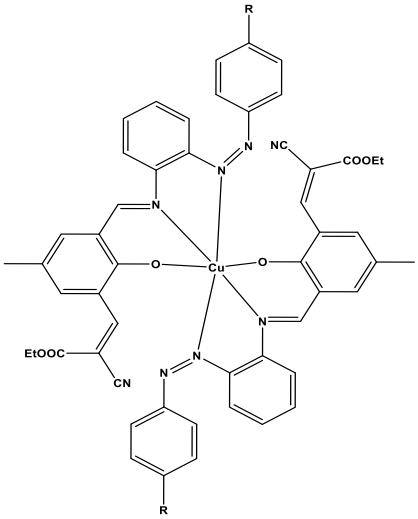 R= H, CH_3 or Cl.	0.230mmol of copper acetate in 5ml of methanol was added to 0.456mmol of ethyl (E)-2-cyano-3-(2-hydroxy-5-methyl-3-((E)-((2-((Z)-phenyldiazenyl)phenyl)imino)methyl)phenyl)acrylate, ethyl (E)-2-cyano-3-(2-hydroxy-5-methyl-3-((E)-((2-((Z)-p-tolyldiazenyl)phenyl)imino)methyl)phenyl)acrylate or ethyl (E)-3-(3-((E)-((2-((Z)-(4-chlorophenyl)diazenyl)phenyl)imino)methyl)-2-hydroxy-5-methylphenyl)-2-cyanoacrylate. The mixture was stirred for 2 hours and the precipitating dark brown product was filtered off and washed with petroleum ether and hexane. Recrystallization was done using dichloromethane and hexane mixture.[90]

18	Figure 46 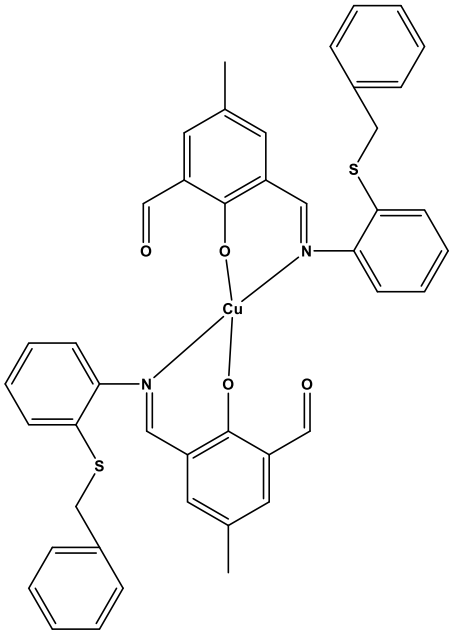	1mmol of 3-((2-(benzylthio)phenylimino)methyl)-2-hydroxy-5-methylbenzaldehyde was added to 1mmol of $Cu(OAc)_2.H_2O$ in 25ml of methanol. The mixture was then stirred for 4 hours at ambient temperature, then it was kept for crystallization.[91]
19	Figure 47 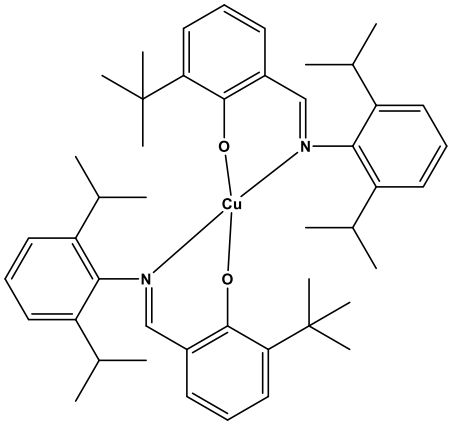	1.0mmol of (E)-2-(*tert*-butyl)-6-(((2,6-diisopropylphenyl)imino)methyl)phenol and 0.5 mmol of copper acetate monohydrate dissolved in 20ml of methanol and refluxed for 4 hours under nitrogen atmosphere. Solid precipitate formed during the reflux. The mixture was cooled to 0°C for 15 minutes and then isolation of the sloid was done using by vacuum filtration. Green crystals were obtained by slow diffusion of ethanol into dichloromethane solution of the complex at -4°C.[92]

20	Figure 48 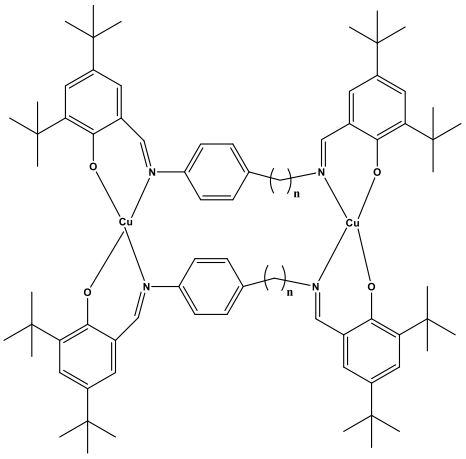 n= 1 or 2.	To 2.00mmol of 6,6'-((1E,1'E)-(((2E,4E)-2-methylhexa-2,4-diene-1,5-diyl)bis(azaneylylidene))bis(methaneylylidene))bis(2,4-di-*tert*-butylphenol) or 6,6'-((1E,1'E)-(((3E,5E)-3-methylhepta-3,5-diene-1,6-diyl)bis(azaneylylidene))bis(methaneylylidene))bis(2,4-di-*tert*-butylphenol) in 25ml of acetonitrile, 4mmol of trimethylamine was added. Then, 2.12mmol of $CuCl_2.2H_2O$ in 5ml of acetonitrile was added to the reaction mixture, which turned into brown colour, and was stirred for 24 hours. Precipitated brown solid was filtered of and washed with acetonitrile then dried. Recrystallization was done with dichloromethane and acetonitrile mixture.[93]
21	Figure 49 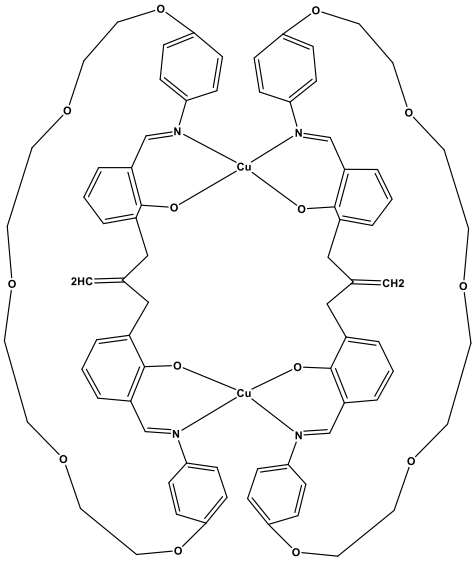	0.1mmol of copper(II) acetate monohydrate was in 25ml of methanol was added to 0.1mmol of (2E,9E)-6-methylene-12,15,18,21,24-pentaoxa-2,10-diaza-1,11(1,4),4,8(1,3)-tetrabenzenacyclotetracosaphane-2,9-diene-42,82-diol in 25ml of chloroform and left without stirring at 25°C for several hours. the resulting precipitate was filtered off.[94]

22	Figure 50 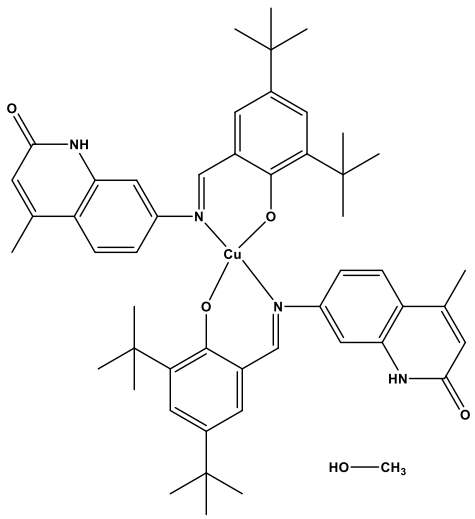	0.0227mmol of copper(II) acetate was dissolved in 30ml of methanol then added drop wise to 0.2500mmol of (7E)-7-(3,5-di-*tert*-butyl-2-hydroxybenzylideneamino)-4-methylquinolin-2(1H)-one dissolved in hot methanol and refluxed for 5 hours until precipitate formed.[95]
23	Figure 51 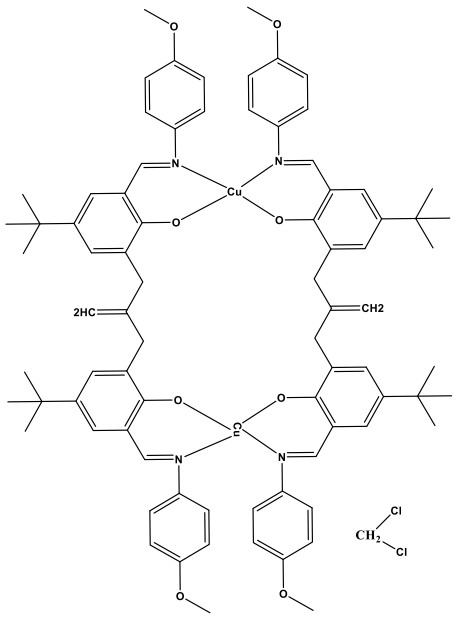	To 0.2mmol of bis(hydroxy benzaldehyde) and 0.2 of dianiline in 10ml chloroform, 0.2mmol of copper(II) acetate monohydrate in 10ml methanol was added. The mixture was left without stirring at 25°C for several minutes then it turned into brown emulsion. A membrane filter was used to filter the emulsion. The residue was washed with chloroform and methanol and then dried in air.[96]

24	Figure 52 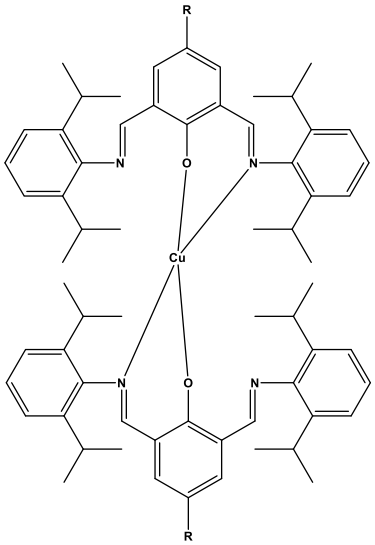 R= Me or Cl.	1.0mmol of 2,6-diformyl-4-methyl-phenoxy(2,6-diisopropylaniline) or 2,6-diformyl-4-chloro-phenoxy(2,6-diisopropylaniline) and 1.0mmol of copper diacetate refluxed in 30ml of toluene for 12 hours. The solvent is then removed under reduced pressure and the residue is extracted into 25ml of hot ethanol or acetonitrile. Green/yellow crystals grew after prolonged standing in room temperature.[97]
25	Figure 53 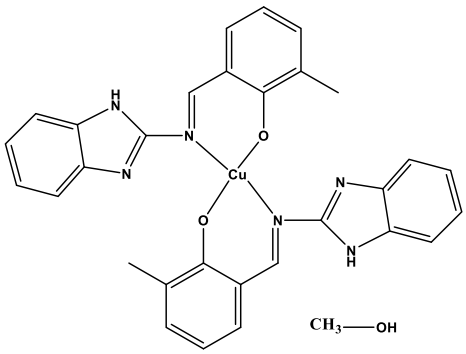	To a filtered solution of 2mmol of (E)-2-(((1H-benzo[d]imidazol-2-yl)imino)methyl)-6-methylphenol and 2mmol of potassium hydroxide in 80ml of methanol, 1mmol of $Cu(OAc)_2.4H_2O$ in 20ml methanol was added. The complex started to crystalize over 24 hours.[98]

Chapter 2

Results and discussion

2.1 Aims

In this chapter, the synthesis of the [2+2] Schiff-base macrocycles and their copper Schiff-base complex will be presented. The crystal structure of each of each compound will be discussed. Detailed synthesis and characterization is presented in chapter 3.

2.2 [2+2] macrocyclic Schiff-base from 2,2'-oxydianiline and 4-*tert*-butyl-2,6-diformylphenol:

Following the published work of Yang *et al.*[7], equimolar amounts of 2,2'-oxydianiline and 4-*tert*-butyl-2,6-diformylphenol were refluxed in methanol (100 ml) in the presence of a few drops of formic acid using Dean-Stark apparatus for 3 hours resulted in a red solution. The solvent was removed under reduced pressure and the residue was dissolved in acetonitrile and kept at ambient temperature for crystals to grow. Upon prolonged standing, orange crystals suitable for single crystal X-ray diffraction have been grown (figures 54-56). X-ray diffraction data is included in the appendix.

The crystal has unique unit cell dimensions which differs from the crystal structure reported by Yang *et al.*[7] The acetone grown crystal has close dimensions to the crystal presented here. Table 6 contain full comparison of the different crystals.

Table 6. A comparison of the crystallographic data between the crystal presented here (**1**) and the crystals reported by Yang et al.[7]

Compound	L.2(MeCN) **1**	L.MeCN **2**	L.MeCOOEt **3**	L.2(MeCOOEt) **4**	L.2(Me_2CO) **5**	L.2(PhMe) **6**
Formula	$C_{48}H_{44}$-$N_4O_4.2(C_2H_3N)$	$C_{48}H_{44}$-$N_4O_4.C_2H_3N$	$C_{48}H_{44}$-$N_4O_4.C_4H_8O_2$	$C_{48}H_{44}$-$N_4O_4.2(C_4H_8O_2)$	$C_{48}H_{44}$-$N_4O_4.2(C_3H_6O)$	$C_{48}H_{44}$-$N_4O_4.2(C_7H_8)$
Formula weight	822.98	781.92	828.97	917.08	857.02	925.14
Crystal system	Monoclinic	Triclinic	Monoclinic	Monoclinic	Monoclinic	Monoclinic
Temperature (K)	100(2)	140(2)	120.0(2)	120.0(2)	293(2)	130.0(1)
Unit cell dimensions						
a (Å)	24.7426(2)	15.1737(5)	24.8335(10)	24.9034(15)	24.5582(10)	13.8127(5)
b (Å)	11.41100(10)	15.3473(6)	11.2046(4)	11.5371(6)	12.1677(7)	16.8060(6)
c (Å)	15.79340(10)	19.2180(7)	15.9714(11)	16.9261(12)	16.0892(7)	22.5196(9)
α (°)	90	98.169(13)	90	90	90	90
β (°)	99.6840(10)	109.862(3)	101.497(6)	96.003(6)	98.942(4)	105.428(4)
γ (°)	60	91.656(3)	90	90	90	90
Crystal size (mm^3)	0.190 x 0.120 x 0.025	0.38 × 0.29 × 0.10	0.49 × 0.40 × 0.38	0.48 × 0.42 × 0.27	0.20 × 0.20 × 0.30	0.50 × 0.40 × 0.30
Cleft angle* (°)	7	13 and 15	17	7	8	89

L= $C_{48}H_{44}N_4O_4$.

*Cleft angle is the angle subtend between the mean planes of the two phenolate rings.

The crystals share some similar characteristics such as being all monoclinic except for **2** which is triclinic. Distances along *a* axes are very close for **1**, **3**, **4** and **5**, but **2** and **6** are shorter then the rest with **6** being the shortest. The *b* axes distances for **1**, **3**, **4** and **5** are shorter the rest with **3** being the shortest and **6** being the longest. The *c* axes distances close for **1, 3, 4** and **5** with **1** being the shortest and **6** the longest. The α angles were similar for all the crystals except **2** which is wider then the rest. The β angles were different for all the crystals with **2** being the widest and **4** being the narrowest. The γ angles were similar for **3-6**, with **2** being close but **1** is much narrower the the rest. The crystal size for **1** is smaller then the others. The cleft angles were the same for **1** and **4** with **5** being very close, **2** and **3** being a little wider and **6** being much wider then the rest.

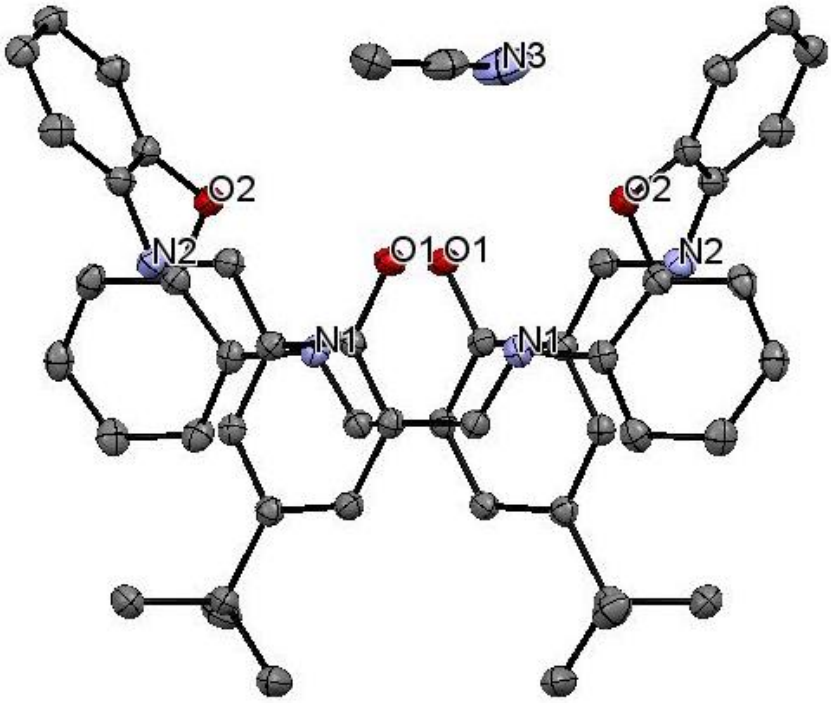

Figure 54. Crystal structure of the [2+2] macrocyclic Schiff-base from 2,2'-oxydianilin and 4-*tert*-butyl-2,6-diformylphenol.

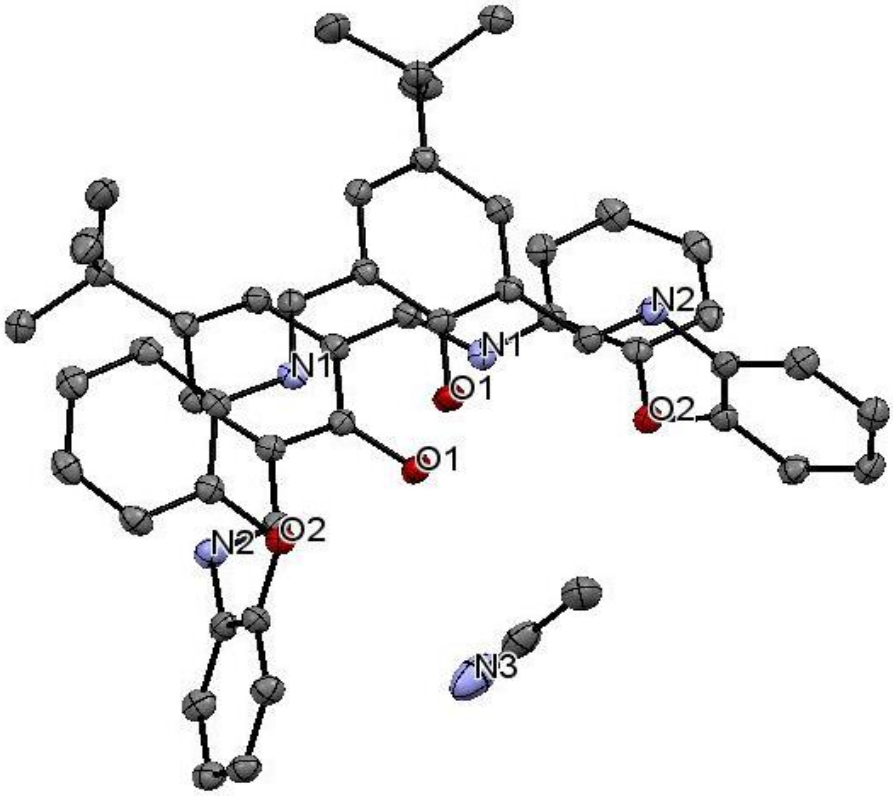

Figure 55. Crystal structure of the [2+2] macrocyclic Schiff-base from 2,2'-oxydianiline and 4-*tert*-butyl-2,6-diformylphenol from a different angle.

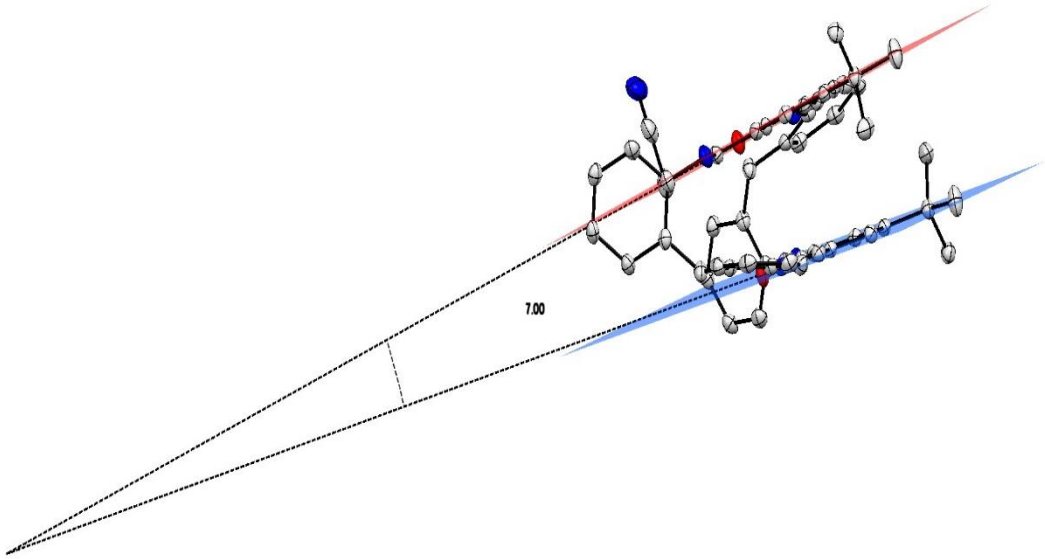

Figure 56. [2+2] macrocyclic Schiff-base from 2,2'-oxydianiline and 4-*tert*-butyl-2,6-diformylphenol showing the cleft angle (7o).

2.3 [2+2] Schiff-base macrocycle from 3,5-diformyl-4-hydroxybenzoic acid and 2,2'-oxydianiline:

The same synthetic route used for [2+2] macrocyclic Schiff-base from 2,2'-oxydianiline and 4-*tert*-butyl-2,6-diformylphenol was used here with substituting 4-*tert*-butyl-2,6-diformylphenol with 3,5-diformyl-4-hydroxybenzoic acid. The resulting product (figure 57) was an orange solid in high yield. Crystallization was attempted using methanol, ethanol, acetonitrile, toluene and dimethylformamide but with no success. However, elemental analysis, ^{1}H NMR spectroscopy, IR and mass spectrometry proved the success of the reaction. The elemental analysis values were consistent with the $C_{42}H_{28}N_4O_8.CH_3OH$ formula. The ^{1}H NMR had peaks on 15.85ppm, 12.71ppm, 9.65ppm and 8.07-7.10ppm for *Ar-OH, COOH, CH=N* and *Ar-OH* respectively. The relative integrations of the ^{1}H NMR peaks are consistent with the proposed formula. The macrocycle has good purity. Full data of elemental analysis, ^{1}H NMR spectra and mass spectrometry are presented in the experimental section.

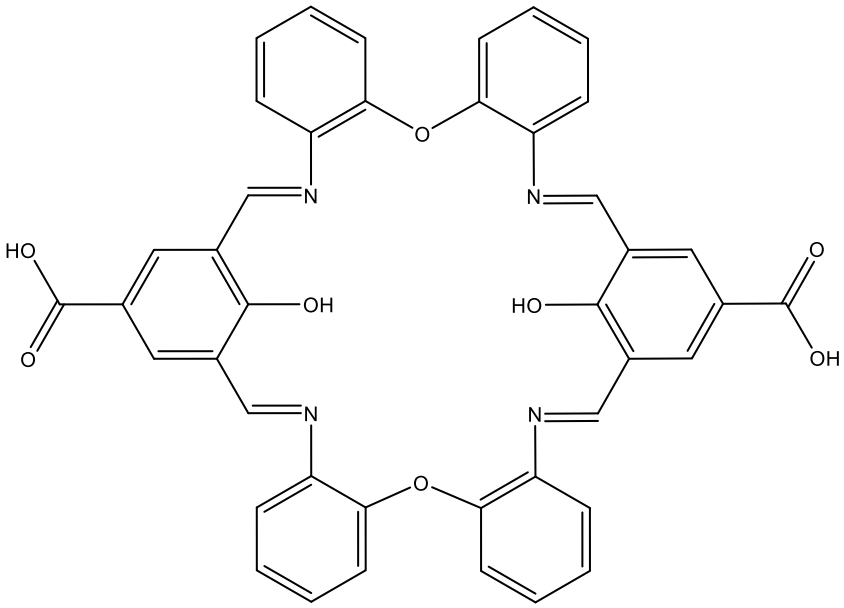

Figure 57. [2+2] Schiff-base macrocycle from 3,5-diformyl-4-hydroxybenzoic acid and 2,2'-oxydianiline.

2.4 Copper Schiff-base complex:

First, the Schiff-base was created by dissolving equimolar amounts of 2-hydroxy-5-methylisophthalaldehyde and 4-aminobenzoic acid in methanol with a few drops of formic acid. After few days in the freezer, the Schiff-base is isolated by filtering and dried under reduced pressure. The ^{1}H NMR showed singlet peaks on 13.98ppm for the *Ar-OH*, 10.40ppm for *COOH*,10.18ppm for *Ar-CH=O* and 9.05ppm for *Ar-CH=N*. It also show multiple peaks on 8.02-7.51ppm for the aromatic *H* and on 2.29ppm for *Ar-CH3*. The relative integrations of the ^{1}H NMR peaks are consistent with the proposed formula. The elemental analysis results were consistent with the $C_{16}H_{13}O_4N$ formula. The purity of this Schiff-base is good.

Copper(II) acetate was reacted with two equivalents of the (E)-4-((3-formyl-2-hydroxy-5-methylbenzylidene)amino)benzoic acid in dimethylformamide (DMF). The mixture was refluxed for 12 hours then the solvent was removed under reduced pressure. Single orange crystals suitable for X-ray diffraction were obtained upon prolonged standing in dimethylformamide at ambient temperature (figure 58). Elemental analysis data are presented in the experimental section.

In the molecular structure, the copper atom lies on a centre of symmetry. The two ligands are coordinated in chelating mode in an approximately square planar pattern. The acid hydrogen atom, H(741), was located in a difference map and refined freely; it forms a hydrogen bond to O(81) of the DMF molecule.

There are indications of disorder in the DMF molecule: a small difference peak was refined as O(86), an alternative to the carbonyl O(81), and this is within a good hydrogen bonding distance from O(742); the (part-occupancy) hydrogen atom on O(742) was not observed. Full X-ray diffraction data is attached to the appendix.

The crystallographic structure show similarities when compared to other copper phenoxy-imine complexes. A check of the Cambridge crystallography data centre website on the November 1st 2018 revealed 46 hits (see table 7 for the most notable hits).

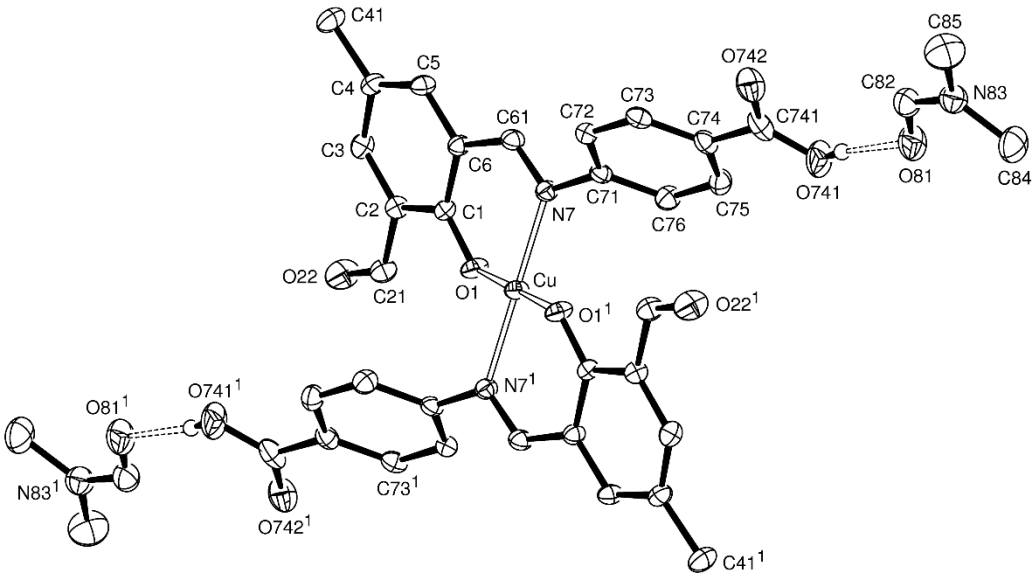

Figure 58. Molecular structure of the copper Schiff-base complex. Selected bonds length (Å) and angles (°): Cu-O(1) 1.8866(11), Cu-N(7) 1.9988(14); O(1)-Cu-N(7) 90.73(5), O(1)-Cu-N(7') 89.27(5).

Table 7. A comparison between the copper complex reported here (#) and other copper phenoxy-imine complexes revealed by the Cambridge crystallography data centre website search on November 1st 2018.[75-98]

	Phenoxy-imine copper complex molecular structure	**Coordination geometry**	**Selected angles (º)**	**Selected bond lengths (Å)**
#	Figure 59 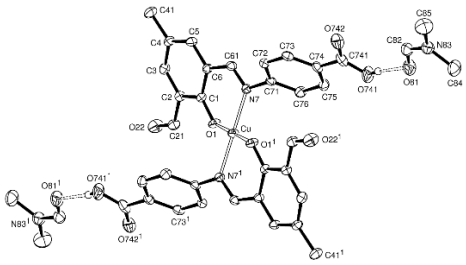	Square planar pattern.	O(1)-Cu-N(7) 90.73(5) O(1)-Cu-N(7') 89.27(5)	Cu-O(1) 1.8866(11) Cu-N(7) 1.9988(14)
1	Figure 60 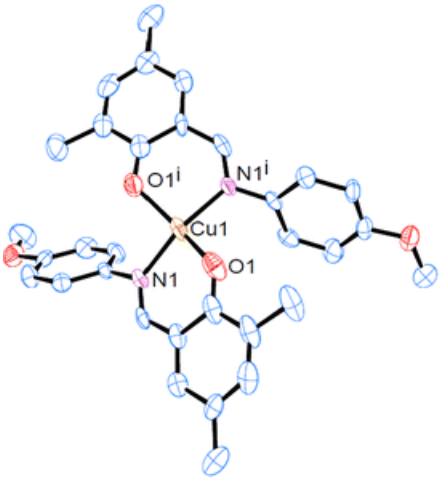 **L1** 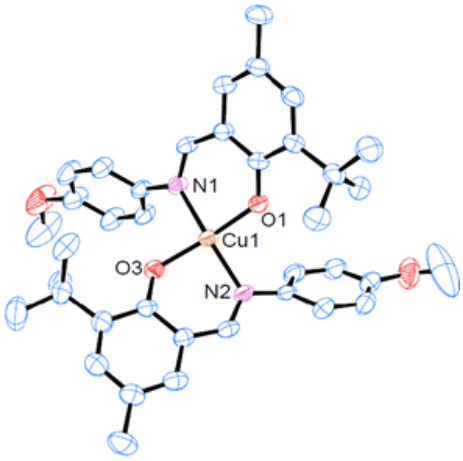 **L2**	L1,L2 and L4 *trans* configuration. L3 perfect square-planer.[75]	L1: Cu–O 1.921 (10) Cu–N 1.968 (9) L2: Cu–O 1.899 (3), 1.889 (3) Cu–N 1.982 (4), 1.972 (4) L3: Cu–O 1.896 (3) Cu–N 1.990 (3) L4: Cu–O 1.896 (5), 1.897 (3) Cu–N 1.947 (7), 1.983 (7)	L1: O–Cu–O 152.4 (7) N–Cu–N 153.5 (6) O-Cu-N[a] 93.1 (4) O-Cu-N 93.1 (4) L2: O–Cu–O 156.33 (17) N–Cu–N 161.73 (19) O-Cu-N[a] 92.32 (16)/92.03 (15) O-Cu-N 91.46 (15)/91.66 (16) L3: O–Cu–O 179.999 (1) N–Cu–N 180.0 O-Cu-N[a] 92.05 (13) O-Cu-N 87.95 (13) L4: O–Cu–O 155.2(2) N–Cu–N 158.8(3) O-Cu-N[a] 92.2(2)/92.3(2) O-Cu-N 93.5(2)/91.0(2)

	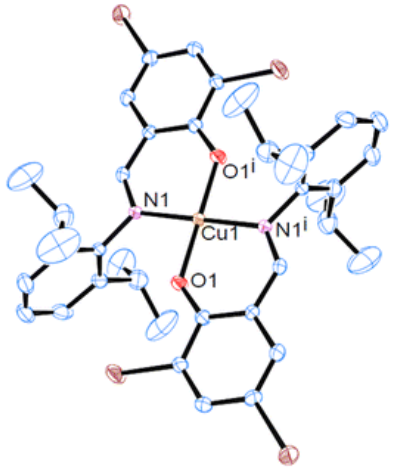 **L3** 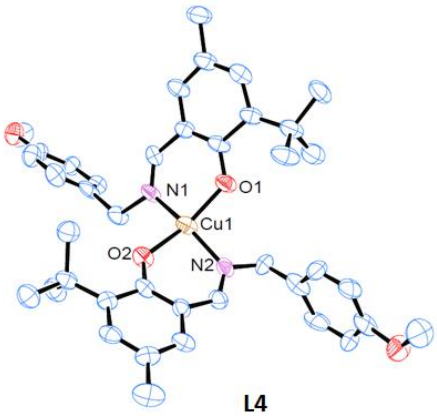 **L4**			
2	Figure 61 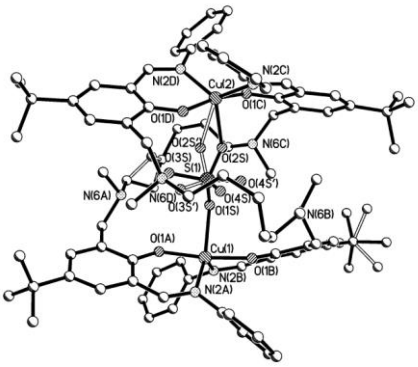	Distorted trigonal-bipyramidal coordination.[76]	O(1B)–Cu(1)–N(2B) 91.3(2) O(1A)–Cu(1)–N(2A) 91.5 (2) O(1D)–Cu(2)–N(2C) 92.7(2) O(1C)–Cu(2)–N(2D) 91.7(2)	Cu(1)–O(1B) 1.899(4) Cu(1)–O(1A) 1.901(4) Cu(1)–N(2A) 2.026(5) Cu(1)–O(1S) 2.165(4) Cu(1)–N(2B) 2.083(5) Cu(2)–O(1D) 1.870(5) Cu(2)–N(2D) 2.064(5) Cu(2)–O(1C) 1.880(5) Cu(2)–N(2C) 2.066(5) Cu(2)–O(2S') 2.305(8)

				Cu(2)–O(2S) 2.188(10)
3	Figure 62 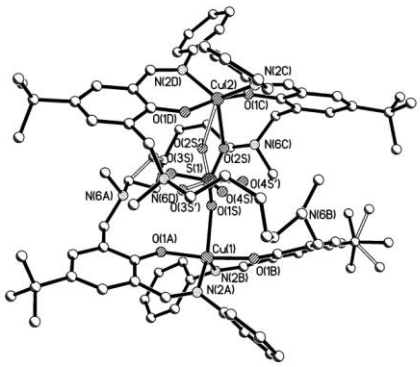	Distorted square-planar coordination.[77]	O1–Cu1–O2 158.5(1) N1–Cu1–N2 160.3(1)	O1–Cu1 1.875(3) O2–Cu1 1.874(3) N1–Cu1 1.995(3) N2–Cu1 1.999(3)
4	Figure 63 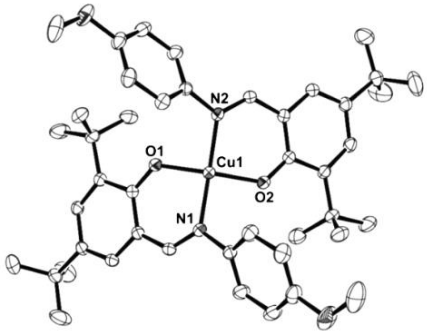	Distorted square planar.[78]	O(1)–Cu–N(1) 93.25(7) O(1)–Cu–N(2) 91.92(7) O(2)–Cu–N(2) 92.91(7) O(2)–Cu–N(1) 92.06(7) O(1)–Cu–O(2) 152.19(9) N(1)–Cu–N(2) 158.77(8)	Cu-O(1) 1.892(4) Cu-O(2) 1.887(2) Cu-N(1) 1.966(2) Cu-N(2) 1.970(2)
5	Figure 64 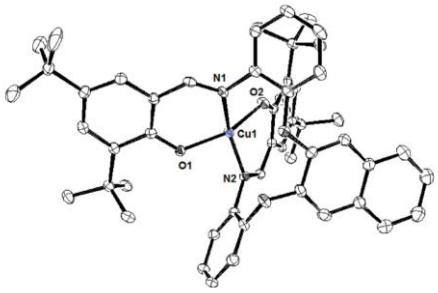	Distorted square planar.[79]	O(1)–Cu(1)–O(2) 151.58(7) O(1)–Cu(1)–N(1) 93.40(8) O(2)–Cu(1)–N(1) 90.32(8) O(1)–Cu(1)–N(2) 92.51(8) O(2)–Cu(1)–N(2) 91.75(8) N(1)–Cu(1)–N(2) 163.57(8)	Cu(1)–O(1) 1.9057(17) Cu(1)–O(2) 1.9148(17) Cu(1)–N(1) 1.959(2) Cu(1)–N(2) 1.9761(19)

6	Figure 65 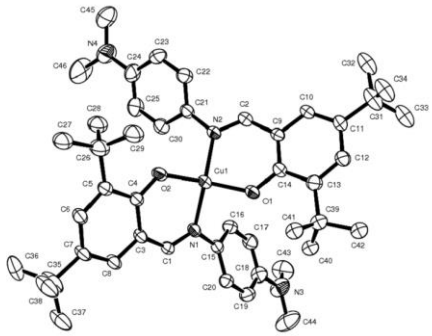	Compressed tetrahedral trans-[CuN_2O_2] coordination.[80]	O1–Cu1–O2 144.2(2) O1–Cu1–N1 93.7(2) N1–Cu1–O2 93.6(2) N2–Cu1–O1 94.4(2) O2–Cu1–N2 97.5(2) N1–Cu1–N2 148.4(2)	Cu1–O1 1.875(4) Cu1–O2 1.882(4) Cu1–N1 1.959(5) Cu1–N2 1.977(5)
7	Figure 66 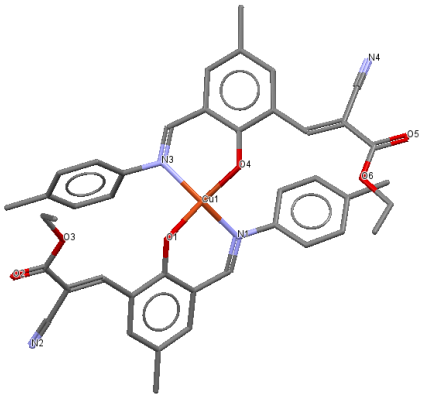	_____[81]	O1-Cu1-N1 93.48(11) O1-Cu1-N3 92.14(11) O4-Cu1-N3 93.17(11) Cu1-O1-C1 129.4(2) Cu1-N1-C13 122.3(2) Cu1-N1-C14 120.1(2)	Cu1-N1 1.981(3) Cu1-N3 1.976(3) Cu1-O1 1.873(2) Cu1-O4 1.883(2)
8	Figure 67 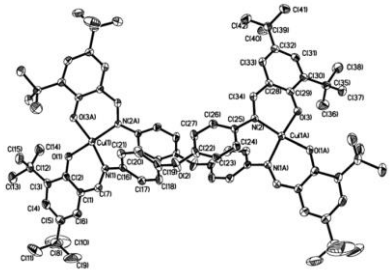	Pseudo-tetrahedral coordination geometry.[82]	O(1)–Cu(1)–O(3)[a] 89.4(1) O(1)–Cu(1)–N(1) 92.6(1) O(3)–Cu(1)–N(1) 147.5(1) O(3)–Cu(1)–N(2)a 93.7(1) O(1)–Cu(1)–N(2)[a] 150.0(1) N(1)–Cu(1)–N(2)[a] 100.5(1)	Cu(1)Cu(1A)[a] 11.66 Cu(1)–O(1) 1.889(2) Cu(1)–O(3)[a] 1.881(2) Cu(1)–N(1) 1.958(3) Cu(1)–N(2)[a] 1.956(3)

9	Figure 68 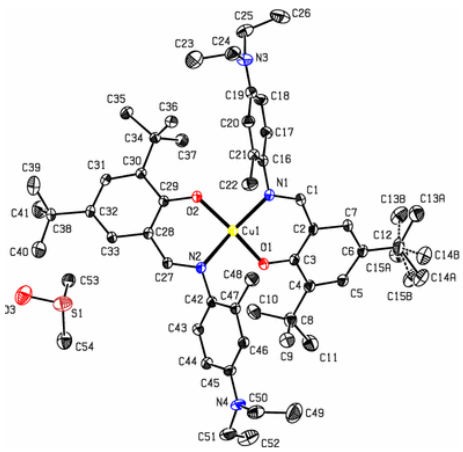	Compressed tetrahedral trans-[N_2O_2] environment.[83]	N1–Cu1–O2 92.6(2) N1–Cu1–O1 93.0(2) N2–Cu1–O1 91.0(2) N2–Cu1–O2 93.2(2)	Cu1–O1 1.904(4) Cu1–O2 1.918(4) Cu1–N1 1.985(5) Cu1–N2 1.994(4)
10	Figure 69 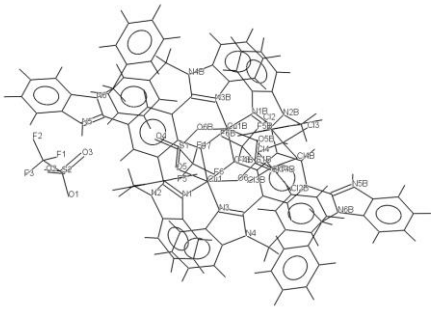	Octahedral geometry.[84]	N1-Cu1-N3 102.13 N3-Cu1-O7B 87.64 N1-Cu-O6 87.75 N1-Cu1-O7 89.15 O5-Cu1-N1 91.30 O5-Cu1-O6 160.47 O7-Cu1-O7B 81.05	Cu1-N3 1.938 Cu1-O6 2.635 Cu1-O7B 1.967 Cu1-O7 1.989 Cu1-O5 2.361 Cu1-N1 1.942 Cu-O6
11	Figure 70 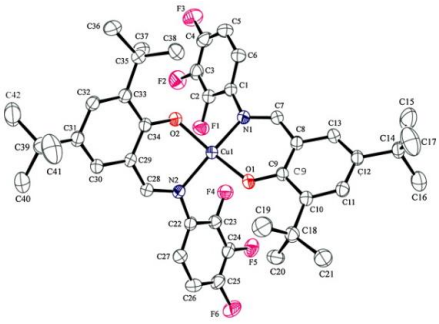	Tetrahedrally distorted square-planar trans-[CuN_2O_2] coordination geometry.[85]	O2–Cu1–O1 151.83(12) O2–Cu1–N1 92.38(11) O2–Cu1–N2 92.56(11) O1–Cu1–N1 94.00(11) O1–Cu1–N2 94.00(11) N2–Cu1–N1 155.73(12)	N1–Cu1 1.956(3) N2–Cu1 1.969(3) O1–Cu1 1.894(2) O2–Cu1 1.891(2)

12	Figure 71 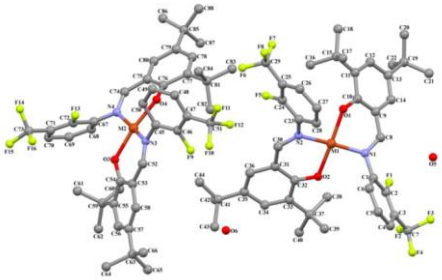	Distorted square-planar coordination geometry.[86]	O2–M1–O1 171.6(2) O1–M1–N1 89.7(2) O1–M1–N2 91.1(2) N1–M1–N2 173.3(2)	N1–Cu 2.011(6) O1–Cu 1.995(5) N2–Cu 2.018(6) O2–Cu 1.995(5)
13	Figure 72 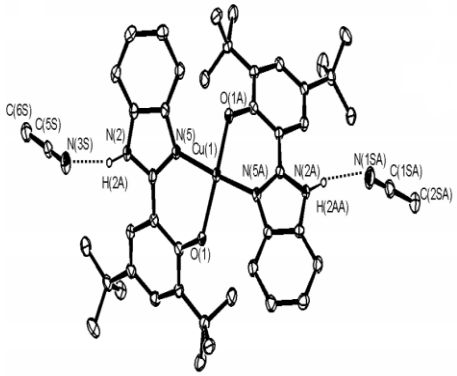	Copper centre possesses an N_2O_2-coordination Sphere.[87]	O(1A)–M(1)–O(1) 155.46(11) N(5A)–M(1)–N(5) 160.66(12) O(1A)–M(1)–N(5) 92.54(11) O(1)–M(1)–N(5A) 93.97(11) O(1A)–M(1)–N(5A) 91.86(11) O(1)–M(1)–N(5) 89.8(1)	Cu–O(1) 1.919(2) Cu–O(1A) 1.898(2) Cu–N(5) 1.947(3) Cu–N(5A) 1.933(3)
14	Figure 73 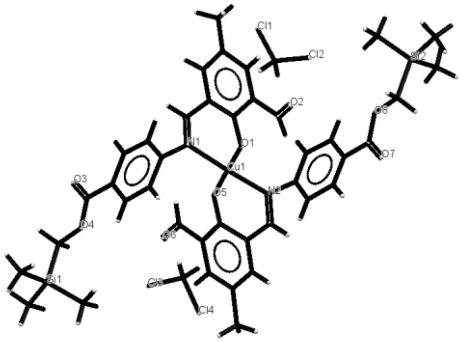	_____[88]	O1–Cu–N1 91.35 O1–Cu–N2 88.91 O5–Cu–N2 89.70 O5–Cu–N1 90.13	Cu–O 1.885(8)– 1.900(8) Cu–N 2.011(8)
15	Figure 74 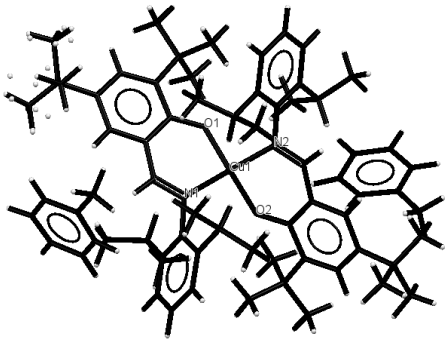	Distorted square planar.[89]	O(1)–Cu–N(1) 93.68(8) O(1)–Cu–N(2) 145.36(9) O(2)–Cu–N(1) 145.36(9) O(2)–Cu–N(2) 93.68(8) O(1)–Cu–O(2) 90.33(8) N(1)–Cu–N(2) 102.05(9)	Cu-O(1) 1.902(2) Cu-O(2) 1.902(2) Cu-N(1) 1.966(2) Cu-N(2) 1.966(2)

16	Figure 75 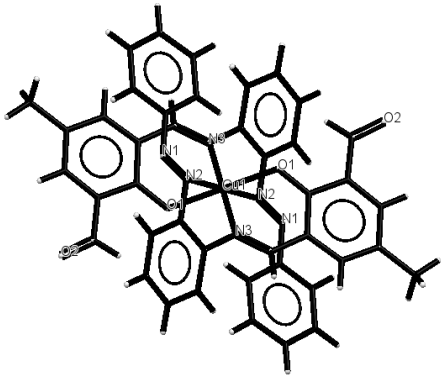	Tetragonally distorted octahedral geometry.[90]	O1-Cu1-N2 105.67(5) O1-Cu1-N3 89.33(5) N2-Cu1-N3 67.99(5)	Cu1-N2 2.7277(15) Cu1-N3 1.9770(14) Cu1-O1 1.9212(10)
17	Figure 76 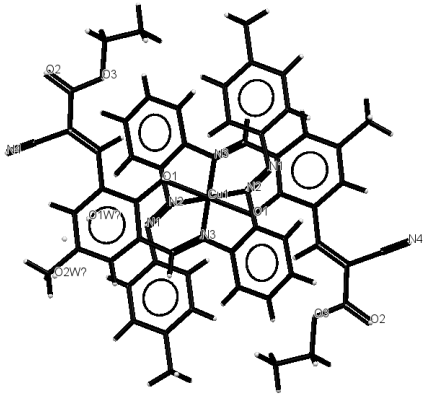	Tetragonally distorted octahedral geometry.[90]	O1-Cu1-N2 102.41(11) O1-Cu1-N3 88.93(12) N2-Cu1-N3 69.16(11)	Cu1-N2 2.644(3) Cu1-N3 1.960(3) Cu1-O1 1.938(3)
18	Figure 77 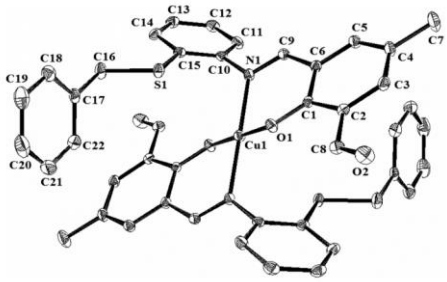	Perfectly square planar CuN_2O_2 coordination.[91]	O1–Cu1–N1 89.38(9) N1–Cu1–N1# 180.00 O1–Cu1–O1# 180.00 O1#–Cu1–N1# 89.38(9) O1–Cu1–N1# 90.62(9)	Cu1–O1 1.905(2) Cu1–N1 2.004(2)

19	Figure 78 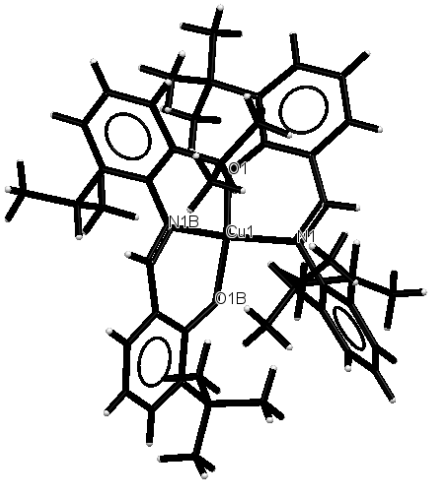 	Distorted square planar geometry.[92]	N-Cu-O 93.13(5) 95.76(5) O-Cu-O 151.42(7) 143.41(8)	Cu-O 1.8959(11) Cu-N 1.9769(13)
20	Figure 79 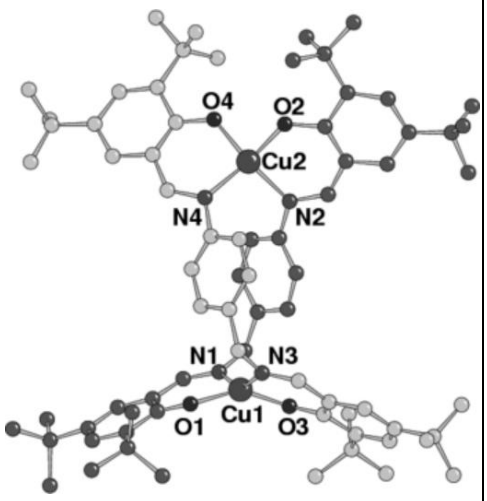 	Severely distorted square-planer to flattened tetrahedral.[93]	O(1)–Cu(1)–O(3) 148.1(3) O(1)–Cu(1)–N(1) 93.5(3) O(2)–Cu(2)–O(4) 88.9(4) O(1)–Cu(1)–N(3) 95.6(3) O(3)–Cu(1)–N(1) 95.6(3) O(2)–Cu(2)–N(4) 149.7(4) O(2)–Cu(2)–N(2) 94.3(4) O(4)–Cu(2)–N(2) 149.7(4) O(3)–Cu(1)–N(3) 93.7(3) N(2)–Cu(2)–N(4) 98.9(4) O(4)–Cu(2)–N(4) 93.2(4) N(1)–Cu(1)–N(3) 145.9(3) Cu1–Cu2 7.687(3)	Cu(2)–O(2) 1.861(9) Cu(1)–O(1) 1.880(7) Cu(1)–O(3) 1.858(7) Cu(1)–N(1) 1.983(8) Cu(2)–O(4) 1.892(8) Cu(2)–N(2) 1.974(10) Cu(2)–N(4) 1.970(10) Cu(1)–N(3) 1.968(8)

21	Figure 80 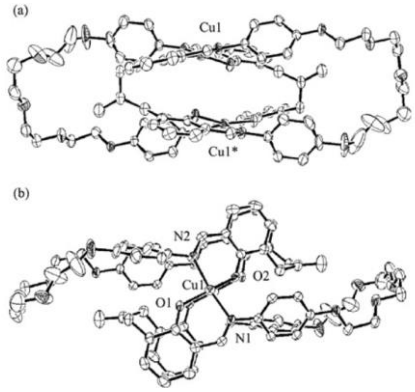	_____[94]	O1−Cu1 1.881 O2−Cu1 1.892 N1−Cu1 2.002 N2−Cu1 1.999 Cu1−Cu1* 4.113	O1−Cu1−O2* 161.0 N1−Cu1−N2 158.6
22	Figure 81 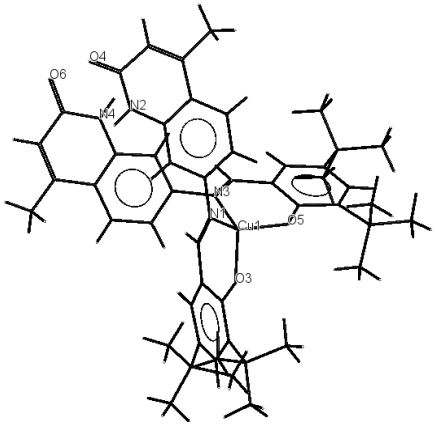	Distorted square planar with significant tetrahedral distortion arrangement.[95]	N1-Cu-N3 104.37 N1-Cu-O3 93.07 O3-Cu-O5 101.43 O5-Cu-N3 92.85	Cu-O5 1.866 Cu-N1 1.919 Cu-O3 1.845 Cu-N3 1.933
23	Figure 82 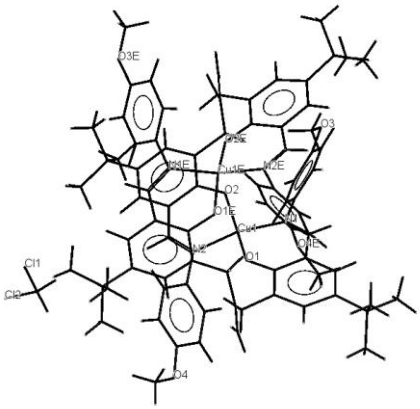	Slightly distorted square-planar coordination.[96]	O1-Cu1-N2 89.80 N2-Cu1-O2 93.13 O2-Cu1-N1 91.15 N1-Cu1-O1 92.99	Cu1-O1 1.864 Cu1-N2 1.984 Cu1-O2 1.880 Cu1-N1 1.991

24	Figure 83 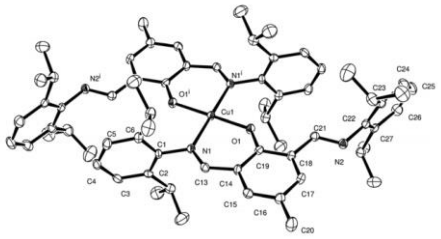	Square planar.[97]	O1–Cu1–N2 91.73(9)	Cu1–O1 1.917(2) Cu1–N1 1.971(2) N1–C13 1.293(4) N2–C22 1.442(4)
25	Figure 84 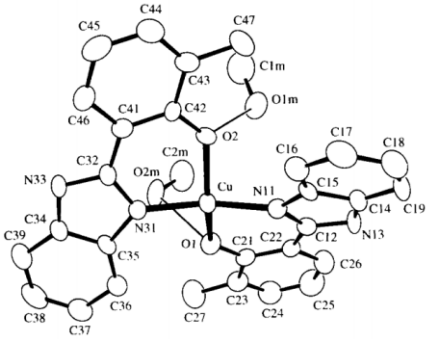	Square-planar geometry.[98]	O(1)-Cu~O(2) 146.0(2) O(1)-Cu-N(I 1) 92.2(2) O(I)-Cu-N(31) 96.0(2) O(2)-Cu-N(11) 92.2(2) O(2)-Cu-N(31) 91.7(2) N(11)--Cu-N(31) 159.2(2)	Cu-O(1) 1.924(4) Cu-O(2) 1.926(4) Cu-N(ll) 1.939(5) Cu-N(31) 1.965(4)

Chapter 3

Experimental

3.1 General Consideration

Manipulations were carried out under an atmosphere of dry nitrogen using conventional Schlenk and cannula techniques or in a conventional nitrogen-filled glove box for the air sensitive reactions. Acetonitrile were refluxed over calcium hydride and toluene was refluxed over sodium. All solvents were distilled and degassed before its use. Nicolet Avatar 360 FT IR spectrometer was used to record IR spectra (nujol mulls, KBr windows). ^{1}H NMR spectra were recorded on a Varian VXR 400 S spectrometer at 400 MHz or a Gemini 300 NMR spectrometer or a Bruker Advance DPX-300 spectrometer at 300 MHz at ambient temperature. The ^{1}H NMR spectra were calibrated toward the deuterated solvent residual protio impurity. Elemental analysis of the chemical compounds was performed by the elemental analysis service at the Chemistry Department of the University of Hull. Trifluoroacetic acid was purchased from fluorochem Ltd. Ethanol, methanol and *n*-hexane were purchased from Honeywell. Hydrochloric acid and formic acid were purchased from Fisher Scientific UK. Acetic acid was purchased from VWR chemicals. Hexamethylenetetramine, 4-*tert*-butyl-2,6-diformylphenol, copper(II) acetate, 2-hydroxy-5-methylisophthalaldehyde and 4-aminobenzoic acid were purchased from sigma Aldrich. 4-hydroxybenzoic acid and 2,2'-oxydianiline were purchased from Alfa Aesar.

3.2 3,5-diformyl-4-hydroxybenzoic acid:

Following the published work of Arafa *et al.*[99] hexamethylenetetramine (9g, 64mmol) and 4-hydroxybenzoic acid (1.1g, 8mmol) were dissolved in 40 ml of trifluoroacetic acid. The mixture was stirred at 110°C for 72 hours, then, it was cooled to ambient temperature and 200mL of 4M HCl was added. It was further stirred for 30 minutes, then it was put aside for precipitate to form. After 3 days the precipitate was isolated by filtration and washed by purified H_2O (3 x 20 mL). It was then dried under reduced pressure. 1.36g of yellow solid was collected and analysed by ^1H NMR spectroscopy and elemental analysis and the results were consistent with what was reported in the literature. (Yield: 62%).

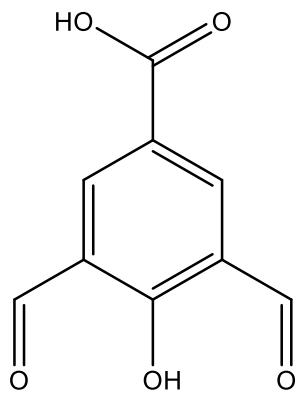

Figure 85. 3,5-diformyl-4-hydroxybenzoic acid.

3.3 [2+2] Schiff-base macrocycle with 3,5-diformyl-4-hydroxybenzoic acid and 2,2'-oxydianiline:

3,5-diformyl-4-hydroxybenzoic acid (670mg, 3.45 mmol) and 2,2'-oxydianiline (690mg, 3.44mmol) were dissolved in 150 mL of ethanol with 10 drops of formic acid. The mixture was refluxed using Dean Stark apparatus which removes the water by-product. Then the solvent was removed under reduced pressure and the resulting oily substance was dissolved in *n*-hexane. The precipitate was filtered and dried under reduced pressure. 2.2 g red solid was collected and analysed by ^{1}H NMR spectroscopy, mass spectroscopy and elemental analysis. (Yield: 89.4%)

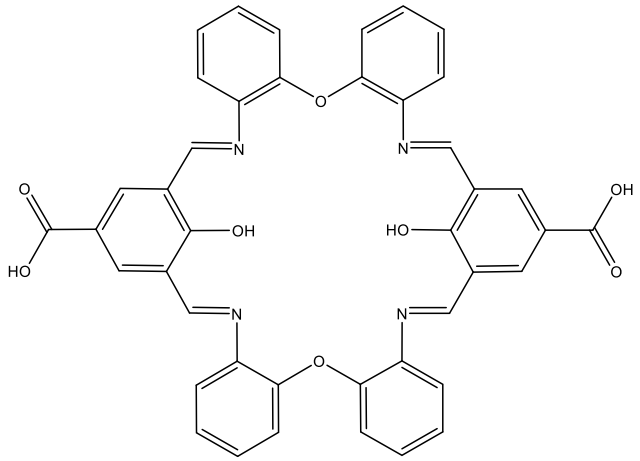

Figure 86. [2+2] Schiff-base macrocycle with 3,5-diformyl-4-hydroxybenzoic acid and 2,2'-oxydianiline.

^{1}H NMR in DMSO-d_6: 15.85 (s, 2H, Ar-OH), 12.71 (s, 2H, COO*H*), 9.65 (s, 4H, Ar-C*H*=N), 8.05-7.10 (m, 20H, Ar-*H*). MALDI-MS m/z= ($C_{42}H_{28}N_4O_8$+DMSO+MeOH) 826. Calculated values for ($C_{42}H_{28}N_4O_8 \cdot CH_3OH$): C 68.98%, H 4.27%, N 7.48; Found: C 68.71%, H

4.16%, N 7.85%. IR (cm^{-1},KBr) 3440 (Ar-OH), 3062 (CO_2H), 1615 (C=N), 1459 (C=C).

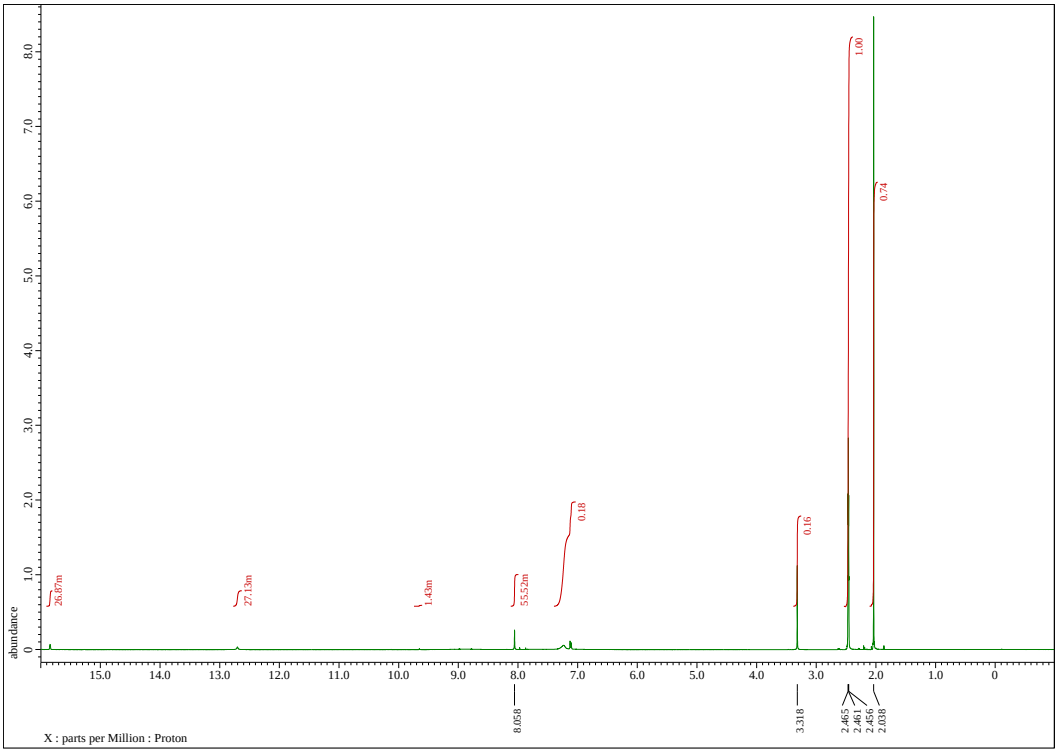

Figure 87. ^{1}H NMR spectrum in DMSO-d_6 for [2+2] Schiff-base macrocycle with 3,5-diformyl-4-hydroxybenzoic acid and 2,2'-oxydianiline.

3.5 Schiff-base with 3,5-diformyl-4-hydroxybenzoic acid and 2,2'-oxydianiline:

A modified method of the published work of Bianchini[100], where 2-hydroxy-5-methylisophthalaldehyde (2.00g, 12.18mmol) and 4-aminobenzoic acid (1.67g, 12.18mmol) were dissolved in 100ml of methanol with 7 drops of formic acid. The mixture was stirred at 0°C for an hour then was placed in the freezer for 48 hours for the product to precipitate. Then, the mixture was filtered and the red solid was dried under reduced pressure at 70°C. (Yield: 82.07%)

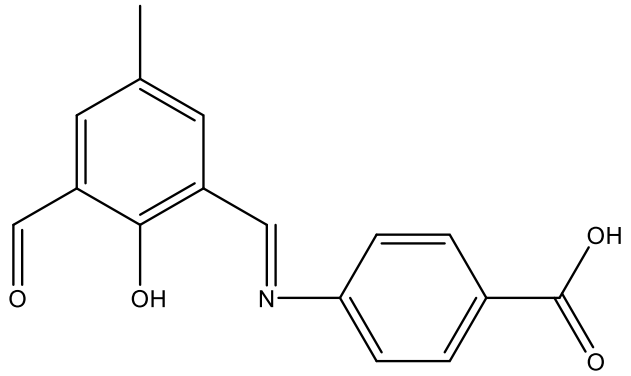

Figure 88. Schiff-base with 3,5-diformyl-4-hydroxybenzoic acid and 2,2'-oxydianiline.

^{1}H NMR in DMSO-d$_6$: 13.98 (s, 1H, Ar-O*H*), 10.40 (s, 1H, COO*H*), 10.18 (s, 1H, Ar-C*H*=O), 9.05 (s, 1H, Ar-C*H*=N), 8.02-7.51 (m, 6H, Ar*H*), 2.29 (m, 3H, C*H*$_3$). Calculated values for: C 67.84%, H 4.63%, N 4.94%; Found: C 67.59%, H 4.78%, N 5.12%.

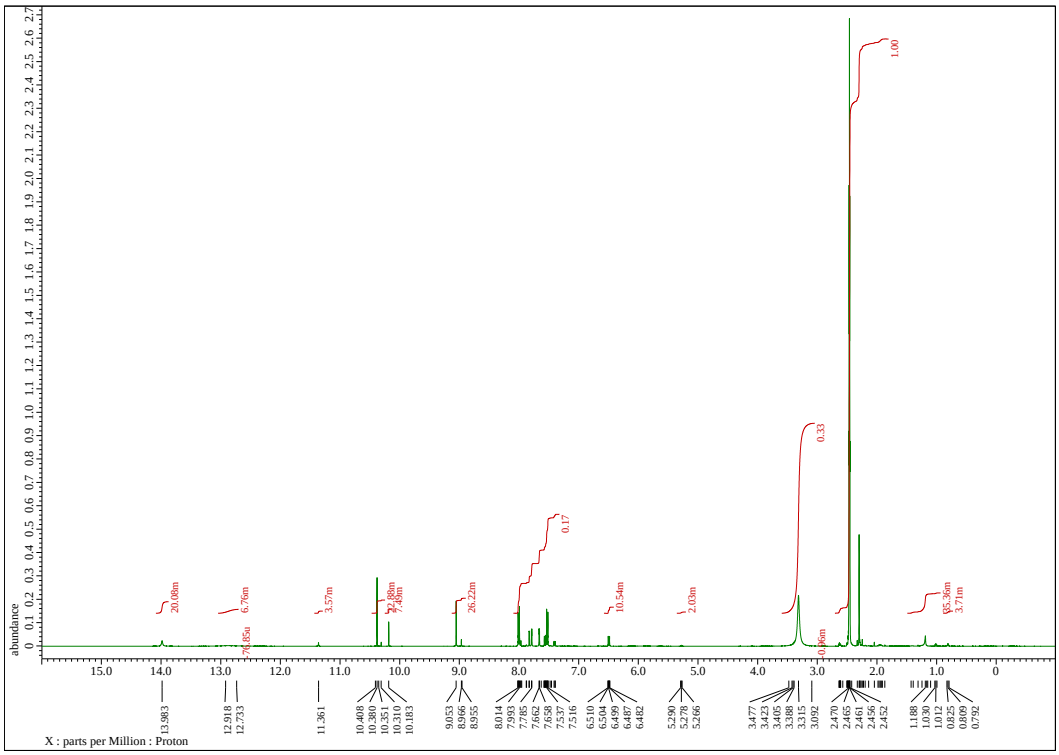

Figure 89. ^{1}H NMR spectrum in DMSO-d$_6$ for Schiff-base with 3,5-diformyl-4-hydroxybenzoic acid and 2,2'-oxydianiline.

3.6 (E)-4-((5-(*tert*-butyl)-3-formyl-2-hydroxybenzylidene)amino)benzoic acid + copper(II) acetate:

(E)-4-((5-(*tert*-butyl)-3-formyl-2-hydroxybenzylidene)amino)benzoic acid (0.5g, 1.5mmol) and of copper(II) acetate (0.137g, 0.75mmol) was dried under reduced pressure at 100°C overnight. Then, 20mL of dry dimethylformamide was added and the mixture was refluxed overnight. Following this, the solvent was removed under reduced pressure and 20mL of dry dimethylformamide was added and the mixture stirred for 5 minutes then filtered and the filtrate was put aside for crystals to grow. (Yield: 12%)

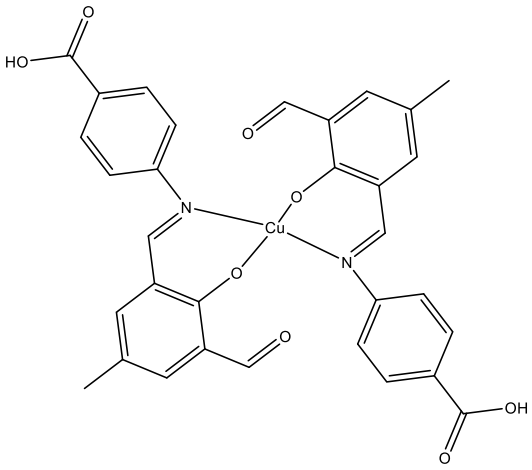

Chemical Formula: $C_{32}H_{24}CuN_2O_8$

Figure 90. (E)-4-((5-(*tert*-butyl)-3-formyl-2-hydroxybenzylidene)amino)benzoic acid + Copper(II) acetate.

Calculated values for $(C_{32}H_{24}CuN_2O_8)\cdot 5C_6H_5CH_3\cdot 6HCON(CH_3)_2$: C 66.68%, H 6.94%, N 7.34% ; Found: C 66.98%, H 5.98%, N 7.57%.

3.4 [2+2] macrocyclic Schiff-base from 2,2'-oxydianiline and 4-*tert*-butyl-2,6-diformylphenol:

4-*tert*-Butyl-2,6-diformylphenol (0.27 g , 1.31 mmol) and 2,2'-oxydianiline (0.262 g , 1.31 mmol) were refluxed in methanol (50 mL) for 4 hours in the presence of 7 drops of acetic acid. After the mixture was cooled to room temperature, the solvent was removed under reduced pressure and the residue was extracted into n-hexane (30ml) and left aside for a week for the solvent to evaporate completely. 1.6 g red solid was obtained. (Yield: 93%)

The results of elemental analysis, mass spectroscopy, IR and ^{1}H NMR spectra were consistent with what was reported previously.[7]

3.5 Conclusion

To summarize, a new Schiff-base macrocycle was developed by refluxing equimolars of 3,5-diformyl-4-hydroxybenzoic acid and 2,2'-oxydianiline in ethanol in the presence of a few drops of formic acid. Although the crystals were never grown successfully, elemental analysis and ^{1}H NMR results prove the success of the reaction. Furthermore, a crystal structure of a known macrocycle made from the refluxing of 4-*tert*-butyl-2,6-diformylphenol and 2,2'-oxydianiline methanol in the presence of drops acetic acid is reported. The results from elemental analysis, IR and mass spectroscopy were consistent with what was reported in literature. Finally, a new copper Schiff-base complex was made by refluxing E)-4-((5-(*tert*-butyl)-3-formyl-2 hydroxybenzylidene)amino)benzoic acid and of copper(II) acetate in dry dimethylformamide. The crystal structure was obtained from crystalizing from dimethylformamide, and reveals square-planer coordination at copper formed via bis(phenoxyimine) ligation.

References

1. A. D. M. a. A. Wilkinson, *IUPAC. Compendium of Chemical Terminology Gold Book*, Blackwell Scientific Publications, Oxford, 1997.
2. J. Kumar, A. Rai and V. Raj, Organic & Medicinal Chem IJ, 2017, 1(3): 555564. DOI: 10.19080/OMCIJ.2017.01.555564.
3. A. M. Abu-Dief and I. M. Mohamed, *BENI-SEUF UNIV. J. APPL. SCI.* 2015, **4**, 119-133.
4. K. Gupta and A. K. Sutar, *Coord. Chem. Rev.* 2008, **252**, 1420-1450.
5. R. Holm, G. Everett Jr and A. Chakravorty, *Prog. Inorg. Chem.* 1966, 83-214.
6. W. Yang, K.-Q. Zhao, B.-Q. Wang, C. Redshaw, M. R. Elsegood, J.-L. Zhao and T. Yamato, *Dalton Trans.* 2016, **45**, 226-236.
7. W. Yang, K.-Q. Zhao, T. J. Prior, D. L. Hughes, A. Arbaoui, M. R. Elsegood and C. Redshaw, *Dalton Trans.* 2016, **45**, 11990-12005.
8. X. Wang, K. Q. Zhao, Y. Al‐Khafaji, S. Mo, T. J. Prior, M. R. Elsegood and C. Redshaw, *Eur. J. Inorg. Chem.* 2017, **2017**, 1951-1965.
9. P. G. Cozzi, *Chem. Soc. Rev.* 2004, **33**, 410-421.
10. E. Canpolat and M. Kaya, *J. Coord. Chem.* 2004, **57**, 1217-1223.
11. M. Yildiz, B. Duelger, S. Koyuncu and B. Yapici, *J. Indian Chem. Soc.* 2004, **81**, 7-12.
12. G. G. Mohamed, M. Omar and A. M. Hindy, *Spectrochim. Acta, Part A: Molecular and Biomolecular Spectroscopy*, 2005, **62**, 1140-1150.
13. A. S. Gaballa, M. S. Asker, A. S. Barakat and S. M. Teleb, *Spectrochim. Acta, Part A: Molecular and Biomolecular Spectroscopy*, 2007, **67**, 114-121.
14. G. G. Mohamed, M. Zayed and S. Abdallah, *J. Mol. Struct.* 2010, **979**, 62-71.
15. M. Tümer, H. Köksal, M. K. Sener and S. Serin, *Transition Met. Chem.* 1999, **24**, 414-420.
16. M. Imran, J. Iqbal, S. Iqbal and N. Ijaz, *Turkish journal of biology*, 2007, **31**, 67-72.
17. N. Raman, S. Johnson Raja and A. Sakthivel, *J. Coord. Chem.* 2009, **62**, 691-709.
18. M. Neelakantan, F. Rusalraj, J. Dharmaraja, S. Johnsonraja, T. Jeyakumar and M. S. Pillai, *Acta, Part A: Molecular and Biomolecular Spectroscopy*, 2008, **71**, 1599-1609.
19. G. Kumar, S. Devi, R. Johari and D. Kumar, *Eur. J. Med. Chem.* 2012, **52**, 269-274.
20. E. Pontiki, D. Hadjipavlou-Litina and A. Chaviara, *J. Enzyme Inhib. Med. Chem.* 2008, **23**, 1011-1017.
21. D. Sriram, P. Yogeeswari, N. S. Myneedu and V. Saraswat, *Bioorg. Med. Chem. Lett.* 2006, **16**, 2127-2129.
22. K. S. Kumar, S. Ganguly, R. Veerasamy and E. De Clercq, *Eur. J. Med. Chem.* 2010, **45**, 5474-5479.
23. S. H. Vincent T DeVita, Steven A Rosenberg, *Cancer: Principles and Practice of Oncology / Edition 7*, Lippincott Williams & Wilkins, New York, 2004.
24. A. A. Vinay Kumar, Nelson Fausto, Richard N Mitchell, *Robbins basic pathology 8th Edition*, SAUNDERS ELSEVIER, Philadilphia 2007.
25. B. P. Bandgar, S. S. Gawande, R. G. Bodade, J. V. Totre and C. N. Khobragade, *Bioorg. Med. Chem.* 2010, **18**, 1364-1370.
26. N. Zhang, Y.-h. Fan, Z. Zhang, J. Zuo, P.-f. Zhang, Q. Wang, S.-b. Liu and C.-f. Bi, *Inorg. Chem. Commun.* 2012, **22**, 68-72.
27. L.-J. Li, C. Wang, C. Tian, X.-Y. Yang, X.-X. Hua and J.-L. Du, *Res. Chem. Intermed.* 2013, **39**, 733-746.

28. M. Hajrezaie, M. Paydar, S. Zorofchian Moghadamtousi, P. Hassandarvish, N. S. Gwaram, M. Zahedifard, E. Rouhollahi, H. Karimian, C. Y. Looi and H. M. Ali, *The Scientific World Journal*, 2014, **2014**.
29. D. L. Bailey and K. P. Willowson, *J Nucl Med*, 2013, **54**, 83-89.
30. L. Livieratos, in *Radionuclide and Hybrid Bone Imaging*, Springer, 2012, pp. 345-359.
31. Y. Ohno, H. Koyama, M. Nogami, D. Takenaka, S. Matsumoto, M. Yoshimura, Y. Kotani and K. Sugimura, *AJR Am. J. Roentgenol*, 2007, **189**, 400-408.
32. O. Israel, R. Hardoff, S. Ish-Shalom, J. Jerushalmi and G. M. Kolodny, *Journal of Nuclear Medicine*, 1991, **32**, 1157-1161.
33. M. M. Ter-Pogossian, M. E. Phelps, E. J. Hoffman and N. A. Mullani, *Radiology*, 1975, **114**, 89-98.
34. J. J. Vaquero and P. Kinahan, Annu. Rev. Biomed. Eng. 2015, **17**, 385-414.
35. A. K. Buck, K. Herrmann, T. Stargardt, T. Dechow, B. J. Krause and J. Schreyögg, *J Nucl. Med. Technol.* 2010, **38**, 6-17.
36. M. E. Marmion, S. R. Woulfe, W. L. Newmann, G. Pilcher and D. L. Nosco, *Nuclear medicine and biology*, 1996, **23**, 567-584.
37. J. L. Lange, D. J. Hayne, P. Roselt, C. A. McLean, J. M. White and P. S. Donnelly, *J. Inorg. Biochem.* 2016, **162**, 274-279.
38. M. Sekerci, C. Alkan and A. Cukurovali, *Russ. J. Inorg. Chem.* 2000, **45**, 1229-1233.
39. M. Figuet, M. T. Averbuch ‐ Pouchot, A. d. M. d'Hardemare and O. Jarjayes, *Eur. J. Inorg. Chem.* 2001, **2001**, 2089-2096.
40. A. A. Khandar, S. A. Hosseini-Yazdi and S. A. Zarei, *Inorg. Chim. Acta,* 2005, **358**, 3211-3217.
41. S. M. Hossain, A. Lakma, R. N. Pradhan, A. Chakraborty, A. Biswas and A. K. Singh, *RSC Advances*, 2015, **5**, 63338-63344.
42. R. E. Mewis and S. J. Archibald, *Coord. Chem. Rev.* 2010, **254**, 1686-1712.
43. M. Wang, L.-F. Wang, Y.-Z. Li, Q.-X. Li, Z.-D. Xu and D.-M. Qu, *Transition Met. Chem.* 2001, **26**, 307-310.
44. A. M. Asiri and S. A. Khan, *Molecules*, 2010, **15**, 6850-6858.
45. M. Maji, M. Chatterjee, S. Ghosh, S. Kumar Chattopadhyay, B.-M. Wu and T. C. W. Mak, *Journal of the Chemical Society, Dalton Trans.* 1999, DOI: 10.1039/A806341I, 135-140.
46. P. Sengupta, R. Dinda, S. Ghosh and W. S. Sheldrick, *Polyhedron*, 2003, **22**, 447-453.
47. P. Banerjee, O. P. Pandey and S. K. Sengupta, *Appl. Organomet. Chem.* 2009, **23**, 19-23.
48. D. Kovala ‐ Demertzi, N. Kourkoumelis, M. A. Demertzis, J. R. Miller, C. S. Frampton, J. K. Swearingen and D. X. West, *Eur. J. Inorg. Chem.* 2000, **2000**, 727-734.
49. N. Raman and C. Thangaraja, *Transition Met. Chem.* 2005, **30**, 317-322.
50. D. Singh and K. Kumar, *Journal of the Serbian Chemical Society*, 2010, **75**, 475-482.
51. U. Kumar and S. Chandra, *Journal of Nepal Chemical Society*, 2010, **25**, 46-52.
52. V. Pawar, S. Joshi and V. Uma, *Biokemistri*, 2011, **23**.
53. R. A. Shiekh, I. Ab Rahman, M. A. Malik, N. Luddin, S. a. M. Masudi and S. A. Al-Thabaiti, *Int. J. Electrochem. Sci*, 2013, **8**, 6972-6987.
54. R. M. Ahmed, E. I. Yousif, H. A. Hasan and M. J. Al-Jeboori, *The Scientific World Journal*, 2013, **2013**.
55. P. Gull and A. A. Hashmi, *J. Braz. Chem. Soc.* 2015, **26**, 1331-1337.

56. M. Singh, *Indian Pharmacopoeia Commission*, 2007.
57. I. Copper, *Dietary reference intakes for vitamin A vitamin K, arsenic, boron, chromium, copper, iodine, iron, manganese, molybdenum, nickel, silicon, vanadium, and zinc*, Washington, DC: The National Academies Press, 2001.
58. S. S. Sadhra, A. D. Wheatley and H. J. Cross, *Sci. Total Environ.* 2007, **374**, 223-234.
59. J. R. Turnlund, R. A. Jacob, C. L. Keen, J. J. Strain, D. S. Kelley, J. M. Domek, W. R. Keyes, J. L. Ensunsa, J. Lykkesfeldt and J. Coulter, *Am. J. Clin. Nutr.* 2004, **79**, 1037-1044.
60. J. R. Turnlund, W. R. Keyes, S. K. Kim and J. M. Domek, *Am. J. Clin. Nutr.* 2005, **81**, 822-828.
61. G. J. Brewer, *J. Am. Coll. Nutr.* 2009, **28**, 238-242.
62. I. Iakovidis, I. Delimaris and S. M. Piperakis, *Molecular Biology International*, 2011, **2011**.
63. M. C. Linder, *Biochemistry of copper*, Springer, 1991, pp. 1-13.
64. M. C. Linder and M. Hazegh-Azam, *Am. J. Clin. Nutr.* 1996, **63**, 797S-811S.
65. E. Frieden, *Clin. Physiol. Biochem.* 1986, **4**, 11-19.
66. C. J. Anderson and R. Ferdani, *Cancer Biotherapy and Radiopharmaceuticals*, 2009, **24**, 379-393.
67. L. A. Bass, M. Wang, M. J. Welch and C. J. Anderson, *Bioconjugate Chem.* 2000, **11**, 527-532.
68. Y. Fujibayashi, H. Taniuchi, Y. Yonekura and H. Ohtani, *J. Nucl. Med.* 1997, **38**, 1155.
69. Y. Fujibayashi, C. Cutler, C. Anderson, D. McCarthy, L. Jones, T. Sharp, Y. Yonekura and M. Welch, *Nucl. Med. Biol.* 1999, **26**, 117-121.
70. J. S. Lewis, R. Laforest, T. L. Buettner, S.-K. Song, Y. Fujibayashi, J. M. Connett and M. J. Welch, *Proc. Natl. Acad. Sci. U.S.A.* 2001, **98**, 1206-1211.
71. J. S. Lewis, R. Laforest, F. Dehdashti, P. W. Grigsby, M. J. Welch and B. A. Siegel, *J. Nucl. Med.* 2008, **49**, 1177-1182.
72. F. Dehdashti, P. W. Grigsby, J. S. Lewis, R. Laforest, B. A. Siegel and M. J. Welch, *J. Nucl. Med.* 2008, **49**, 201-205.
73. E. D. Pressly, R. Rossin, A. Hagooly, K.-i. Fukukawa, B. W. Messmore, M. J. Welch, K. L. Wooley, M. S. Lamm, R. A. Hule, D. J. Pochan and C. J. Hawker, *Biomacromolecules*, 2007, **8**, 3126-3134.
74. K.-i. Fukukawa, R. Rossin, A. Hagooly, E. D. Pressly, J. N. Hunt, B. W. Messmore, K. L. Wooley, M. J. Welch and C. J. Hawker, *Biomacromolecules*, 2008, **9**, 1329-1339.
75. M. Mandal, K. Oppelt, M. List, I. Teasdale, D. Chakraborty and U. Monkowius, *Monatshefte für Chemie-Chemical Monthly*, 2016, **147**, 1883-1892.
76. P. G. Plieger, S. Parsons, A. Parkin and P. A. Tasker, *Journal of the Chemical Society, Dalton Transactions*, 2002, 3928-3930.
77. H. Houjou, A. Iwasaki, T. Ogihara, M. Kanesato, S. Akabori and K. Hiratani, *New Journal of Chemistry*, 2003, **27**, 886-889.
78. B. Chakraborty and S. Banerjee, *J. Coord. Chem.*, 2013, **66**, 3619-3628.
79. H. Keypour, M. Shayesteh, R. Golbedaghi, A. Chehregani and A. G. Blackman, *J. Coord. Chem.*, 2012, **65**, 1004-1016.
80. R. Kilinçarslan, H. Karabiyik, M. Ulusoy, M. Aygün, B. Çetinkaya and O. Büyükgüngör, *J. Coord. Chem.*, 2006, **59**, 1649-1656.
81. S. P. Parua, D. Sinha and K. K. Rajak, *ChemistrySelect*, 2018, **3**, 1120-1128.
82. Z. Chu and W. Huang, *Journal of molecular structure*, 2007, **837**, 15-22.
83. M. Ulusoy, H. Karabıyık, R. Kılınçarslan, M. Aygün, B. Cetinkaya and S. García-Granda, *Struct. Chem.* 2008, **19**, 749-755.

84. Q. T. He, X. P. Li, Y. Liu, Z. Q. Yu, W. Wang and C. Y. Su, *Angew. Chem.* 2009, **121**, 6272-6275.
85. V. T. Kasumov, I. Uçar and A. Bulut, *Journal of J. Fluorine Chem.*, 2010, **131**, 59-65.
86. V. T. Kasumov, O. Sahin and H. G. Aktas, *Polyhedron*, 2016, **115**, 119-127.
87. L. Benisvy, E. Bill, A. J. Blake, D. Collison, E. S. Davies, C. D. Garner, G. McArdle, E. J. McInnes, J. McMaster and S. H. Ross, *Dalton Trans*, 2006, 258-267.
88. M.-F. Zaltariov, M. Cazacu, A. Vlad, L. Sacarescu and S. Shova, *High Perform. Polym.*, 2015, **27**, 607-615.
89. A. Mrutu, A. C. Lane, J. M. Drewett, S. D. Yourstone, C. L. Barnes, C. M. Halsey, J. W. Cooley and J. R. Walensky, *Polyhedron*, 2013, **54**, 300-308.
90. P. Mondal, S. P. Parua, P. Pattanayak, U. Das and S. Chattopadhyay, *J. Chem. Sci.* 2016, **128**, 803-813.
91. P. Pattanayak, J. L. Pratihar, D. Patra, C.-H. Lin, P. Brandão, D. Mal and V. Felix, *J. Coord. Chem.*, 2013, **66**, 568-579.
92. S. Bhunora, J. Mugo, A. Bhaw‐Luximon, S. Mapolie, J. Van Wyk, J. Darkwa and E. Nordlander, *Appl. Organomet. Chem.*, 2011, **25**, 133-145.
93. P. Halder, P. R. Banerjee, E. Zangrando and T. K. Paine, *Eur. J. Inorg. Chem.*, 2008, **2008**, 5659-5665.
94. H. Houjou, N. Schneider, Y. Nagawa, M. Kanesato, R. Ruppert and K. Hiratani, *Eur. J. Inorg. Chem*, 2004, **2004**, 4216-4222.
95. B. S. Creaven, B. Duff, D. A. Egan, K. Kavanagh, G. Rosair, V. R. Thanglela and M. Walsh, *Inorganica Chim. Acta*, 2010, **363**, 4048-4058.
96. H. Houjou, Y. Shimizu, N. Koshizaki and M. Kanesato, *Adv. Mater.*, 2003, **15**, 1458-1461.
97. X. Wang, K.-Q. Zhao, M. R. Elsegood, T. J. Prior, X. Liu, L. Wu, S. Sanz, E. K. Brechin and C. Redshaw, *RSC Advances*, 2015, **5**, 57414-57424.
98. J. D. Crane, R. Hughes and E. Sinn, *Inorganica Chim. Acta*, 1995, **237**, 181-185.
99. W. A. Arafa, M. D. Kärkäs, B.-L. Lee, T. Åkermark, R.-Z. Liao, H.-M. Berends, J. Messinger, P. E. Siegbahn and B. Åkermark, *Phys. Chem. Chem. Phys.*, 2014, **16**, 11950-11964.
100. C. Bianchini, G. Mantovani, A. Meli, F. Migliacci, F. Zanobini, F. Laschi and A. Sommazzi, *Eur. J. Inorg. Chem.*, 2003, **2003**, 1620-1631.
101. Da Silva, C.M., da Silva, D.L., Modolo, L.V., Alves, R.B., de Resende, M.A., Martins, C.V. and de Fátima, Â., 2011. Schiff bases: A short review of their antimicrobial activities. Journal of Advanced research, 2(1), pp.1-8.

Appendix

4.1 Table 7. Crystallographic data of [2+2] macrocyclic Schiff-base from 2,2'-oxydianiline and 4-*tert*-butyl-2,6-diformylphenol:

Empirical formula	$C_{52}H_{50}N_6O_4$	
Formula weight	822.98	
Temperature	100(2) K	
Wavelength	1.54184 Å	
Crystal system	Monoclinic	
Space group	C 2/c	
Unit cell dimensions	a = 24.7426(2) Å	α= 90°.
	b = 11.41100(10) Å	β= 9.6840(10)°.
	c = 15.79340(10) Å	γ= 90°.
Volume	4395.53(6) $Å^3$	
Z	4	
Density (calculated)	1.244 Mg/m^3	
Absorption coefficient	0.634 mm^{-1}	
F(000)	1744	
Crystal size	0.190 x 0.120 x 0.025 mm^3	
Theta range for data collection	3.624 to 68.235°.	
Index ranges	-29<=h<=29, -13<=k<=13, -17<=l<=18	
Reflections collected	19275	
Independent reflections	4013 [R(int) = 0.0252]	
Completeness to theta = 67.684°	99.7 %	
Absorption correction	Semi-empirical from equivalents	
Max. and min. transmission	1.000 and 0.72106	
Refinement method	Full-matrix least-squares on F^2	
Data / restraints / parameters	4013 / 10 / 296	
Goodness-of-fit on F^2	1.048	
Final R indices [I>2sigma(I)]	R1 = 0.0375, wR2 = 0.0989	
R indices (all data)	R1 = 0.0401, wR2 = 0.1009	
Extinction coefficient	n/a	
Largest diff. peak and hole	0.299 and -0.197 $e.Å^{-3}$	

4.2 Table 8. Crystal data and structure refinement for (E)-4-((5-(*tert*-butyl)-3-formyl-2-hydroxybenzylidene)amino)benzoic acid + Copper(II) acetate

Elemental formula	C_{32} H_{24} Cu N_2 O_8, 2(C_3 H_7 N O)
Formula weight	774.3
Crystal system	Monoclinic
Space group	$P2_1/c$ (no. 14)
Unit cell dimensions	a = 15.1396(18) Å α = 90 °
	b = 7.1905(5) Å β = 98.416(9) °
	c = 16.3497(17) Å γ = 90 °
Volume	1760.7(3) Å3
No. of formula units, Z	2
Calculated density	1.460 mg/m^3
F(000)	806
Absorption coefficient	0.687 mm^{-1}
Temperature	140(1) K
Wavelength	0.71073 Å
Crystal colour, shape	Orange prism
Crystal size	0.26 x 0.18 x 0.11 mm
Crystal mounting	On a glass fibre, in oil, fixed
	in cold N_2 stream
On the diffractometer:	
Theta range for data collection	3.5 to 27.5 °
Limiting indices	-19<=h<=19, -9<=k<=9, -21<=l<=21
Completeness to theta = 27.5	99.7 %
Absorption correction	Semi-empirical from equivalents
Max. and min. transmission	1.068 and 0.939
Reflections collected (not including absences)	29426
No. of unique reflections	4035 [R(int) for equivalents = 0.056]
No. of 'observed' reflections	($I > 2\sigma_I$) 3075
Structure determined by:	direct methods, in SHELXS
Refinement:	Full-matrix least-squares on F^2, in SHELXL
Data / restraints / parameters	4035 / 0 / 253
Goodness-of-fit on F^2	0.957
Final R indices ('observed' data)	R_1 = 0.031, wR2 = 0.080
Final R indices (all data)	R_1 = 0.047, wR2 = 0.083
Reflections weighted:	
$w = [\sigma^2(Fo^2)+(0.0514P)^2]^{-1}$ where $P=(Fo^2+2Fc^2)/3$	
Largest diff. peak and hole	0.29 and -0.41 e.Å-3
Location of largest difference peak	on C(74)-C(75) bond